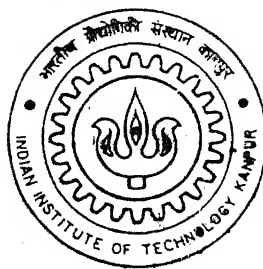


# **EXPERIMENTAL INVESTIGATIONS INTO ELECTRODISCHARGE DIAMOND GRINDING (EDDG)**

By

**Rakesh G. Mote**



**DEPARTMENT OF MECHANICAL ENGINEERING**

**Indian Institute of Technology Kanpur**

**FEBRUARY, 2002**

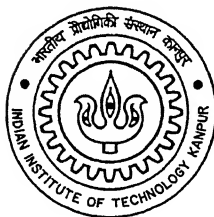
**EXPERIMENTAL INVESTIGATIONS  
INTO  
ELECTRODISCHARGE DIAMOND GRINDING  
(EDDG)**

*A Thesis Submitted  
in Partial Fulfillment of the Requirement  
for the Degree of*

**MASTER OF TECHNOLOGY**

by

**RAKESH G. MOTE**



to the

**DEPARTMENT OF MECHANICAL ENGINEERING  
INDIAN INSTITUTE OF TECHNOLOGY KANPUR  
FEBRUARY, 2002**

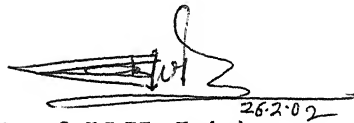
पुरुषोत्तम /ME  
भारतीय प्रौद्योगिकी संस्थान कानपुर  
अवधि क्र० A.....139585



A139585

# CERTIFICATE

It is certified that the thesis work entitled *Experimental Investigations into Electrodischarge Diamond Grinding (EDDG)* by Rakesh G. Mote has been carried out under my supervision, and that it has not been submitted elsewhere for a degree.

A handwritten signature in black ink, appearing to be 'V.K. Jain', written over a horizontal line. Below the line, the date '26.2.02' is written.

(Prof. V.K. Jain)

Department of Mechanical Engineering  
Indian Institute of Technology  
Kanpur 208 016 India

February, 2002

# Acknowledgements

---

I take this opportunity to express the feelings of sincere gratitude towards my thesis supervisor Prof. V. K. Jain for his expert guidance, and encouragement, which has been vital factors in successful completion of the present work. Also, I am indebted to Prof. T.P. Bagchi of Industrial and Management Engineering Department for his motivation and valuable discussions about experimental designs.

I acknowledge the financial support from Council of Scientific and Industrial Research (CSIR), New Delhi for the project *Abrasive Electrodischarge Grinding of Advanced Engineering Materials*.

I am grateful to Mr. Vinod Yadava for clearing my fundamentals of EDDG. Also, assistance provided by Mrs. Anjali Kulkarni, Robotics Department, and Mrs. Lalita, in instrumentation part of the experimentation is of immense help.

Many thanks to Mr. R.M. Jha, Mr. H.P. Sharma and Mr. Namdev for assisting my work even during holidays and at nights also. Special mention of Phoolchand and Rakesh Thapliyal of manufacturing science laboratory for their skillful and friendly rendering of all possible help in setting up and conducting the experiments.

Mr. D.S. Bilgi, Mr. D.K. Singh, Mr. S.C. Jayswal and Mr. V.K. Gorana, Ph.D. scholars, never made me feel away from home. Sincere thanks to their caring attitude and for their valuable, timely advice.

I owe a special debt to my friends here, especially Gaurav, Anil and Sagar. They made my stay at IIT enjoyable and memorable (although I have cleared this debt partially by giving treats to them time to time!).

Lastly, the greatest debt is owed to *nana* (father), *bhabhi* (mother), *didi*, *babloo*, *dada*, *bhaiya* and *vahinis*. Without their encouragement and blessings, this work would not have been possible. Also, special mention of my sweet nephews, Gauri, Gautami, Manasi and Gayatri. The everlasting source of motivation, my life mate, Manisha, whose support during all the days of my struggle I cannot ever adequately acknowledge.

**Dedicated to my parents...**

---

“There are many examples of old, incorrect theories that stubbornly persisted, sustained only by the prestige of foolish but well-connected scientists. ... Many of these theories have been killed off only when some decisive experiment exposed their incorrectness... Thus, the yeoman work in any science, and especially physics, is done by the experimentalist, who must keep the theoreticians honest.”

-**Michio Kaku**, *Hyperspace*, Oxford University Press, 1995, p. 263 (1)

---

# Abstract

---

Combination of two or more machining processes may result in the increase of the productivity. This is an approach worthy to be tried especially for the machining of difficult- to-machine materials. Also, this approach may be fruitful in removing drawbacks of constituent processes. In the present study, a hybrid machining process called “electrodischarge diamond grinding (EDDG)” is under investigation.

Temperature of the workpiece during machining is an important consideration because it introduces thermal stresses into the workpiece. Effect of process parameters (Pulse current, pulse on-time and wheel speed) on temperature of the workpiece was investigated. Scientific tool like experimental design was used for the experimentation. Material removal rate was also taken as response. All the experiments were conducted on CNC EDM machine with special grinding attachment. A regression model was developed describing the relationship between responses and process parameters. It was found that pulse current has dominating effect on temperature and MRR.

Specific energy is a vital consideration for any machining process. EDM is known for its inefficiency. Specific energy was calculated for EDDG. Also, experiments were conducted with a specially fabricated bronze disc to evaluate specific energy in EDM with rotating disc and results were compared with that of EDDG. It has been found that specific EDDG energy is less than that of EDM with rotating disc implying feasibility of the EDDG process.

Evolution of cutting forces with process parameters is an interesting phenomenon. Efforts are made to correlate cutting forces with temperature of the workpiece.

Thus, present thesis may provide some useful input to the technological development of the, comparatively new hybrid process, electrodischarge diamond grinding (EDDG).



# Contents

<b>List of Figures</b>	<b>ix</b>
<b>List of Tables</b>	<b>xii</b>
<b>Nomenclature</b>	<b>xiii</b>
<b>1. Introduction and Literature Review</b>	<b>1</b>
1.1 Introduction	1
1.2 Electrodischarge Diamond Grinding (EDDG)	2
1.3 Literature Survey	5
1.3.1 Electrodischarge Machining and Grinding	5
1.3.2 Hybrid Machining Processes	8
1.3.3 Electrodischarge Diamond Grinding	11
1.4 Scope and Organization of the Thesis	14
1.4.1 Objectives of the Thesis	14
1.4.2 Organization of the Thesis	14
<b>2. Experimentation</b>	<b>16</b>
2.1 Experimental set up	16
2.2 Wheel Truing and Dressing	17
2.3 Design of Experiments (DOE)	19
2.3.1 Model Fitting	22
2.3.2 Analysis of Variance (ANOVA)	23
2.4 Temperature Measurement	24
2.5 Force Measurement	25
2.6 Experimentation for EDM with Rotating Disc	28

<b>3. Parametric Analysis of Temperature and Material Removal</b>	
<b>Rate in EDDG</b>	<b>29</b>
3.1 Experimental Results	29
3.2 Discussion	34
3.2.1 Effect of Pulse Current	36
3.2.2 Effect of Wheel Speed	39
3.2.3 Effect of Pulse on-time	42
<b>4. Specific Energy in EDDG</b>	<b>45</b>
4.1 Specific Energy Calculation	45
4.2 Experimental Results and Discussion	46
4.2.1 Specific EDDG Energy	46
4.2.1.1 Effect of Pulse Current	48
4.2.1.2 Effect of Wheel Speed	49
4.2.1.3 Effect of Pulse On-time	50
4.2.1.4 Effect of Duty Factor	51
4.2.2 Specific energy in EDM with rotating disc	53
4.2.2.1 Comparison of EDDG with EDM	53
<b>5. Conclusions and Scope for Future Work</b>	<b>56</b>
5.1 Conclusions	56
5.2 Scope for Future Work	57
<b>References</b>	<b>59</b>
<b>Appendices</b>	<b>63</b>

# List of Figures

- 1.1 Basic configurations of EDM-grinding hybrid processes (a) Combined dressing and grinding zones, (b) Isolated dressing and grinding zones.
- 1.2 EDDG in surface grinding mode.
- 1.3 EDDG in face grinding mode.
- 1.4 A grit-chip thermocouple circuit.
- 1.5 Selected methods of abrasive electrical machining.
- 2.1 General scheme of electrodischarge diamond grinding.
- 2.2 Different modes of plunge grinding (a) Cut-off grinding (b) Face grinding
- 2.3 Wheel wear in grinding.
- 2.4 Types of interactions.
- 2.5 Specimen geometry used for experimentation.
- 2.6 Octagonal ring type dynamometer for measurement of forces.
- 2.7 Circuit diagrams for measurement of (a)  $F_n$  and (b)  $F_t$ .
- 2.8 Circular strain ring showing the type of deformation produced.
- 2.9 A disc used for EDM experiments.
- 3.1 Sample recorder output.
- 3.2 Main effects model for MRR
- 3.3 Main effects model for temperature.
- 3.4 Pulsed D.C. voltage.
- 3.5 Plasma channel profile during EDM.
- 3.6 Effect of pulse current on (a) Material Removal Rate and (b) Temperature at wheel speed 2.5 m/s.
- 3.7 Effect of pulse current on (a) Material Removal Rate and (b) Temperature at wheel speed 5 m/s.

- 3.8 Effect of pulse current on (a) Material Removal Rate and (b) Temperature at wheel speed 7.5 m/s.
- 3.9 Schematic representation of the wheel-work interface in EDDG.
- 3.10 Effect of wheel speed on (a) Material Removal Rate and (b) Temperature at pulse on-time 100  $\mu$ s.
- 3.11 Effect of wheel speed on (a) Material Removal Rate and (b) Temperature at pulse on-time 200  $\mu$ s.
- 3.12 Effect of wheel speed on (a) Material Removal Rate and (b) Temperature at pulse on-time 300  $\mu$ s.
- 3.13 Effect of pulse on-time on (a) Material Removal Rate and (b) Temperature at pulse current 7 A.
- 3.14 Effect of pulse on-time on (a) Material Removal Rate and (b) Temperature at pulse current 13 A.
- 3.15 Effect of pulse on-time on (a) Material Removal Rate and (b) Temperature at pulse current 19 A.
- 4.1 Effect of pulse current on cutting force and temperature (Wheel speed = 2.5 m/s; pulse on-time = 100  $\mu$ s; duty factor = 0.64; voltage = 40 V).
- 4.2 Effect of pulse current on specific EDDG energy (Wheel speed = 2.5 m/s; pulse on-time = 100  $\mu$ s; duty factor = 0.64; voltage = 40 V).
- 4.3 Effect of wheel speed on cutting force and temperature (Pulse current = 7 A; pulse on-time = 100  $\mu$ s; duty factor = 0.64; voltage = 40 V).
- 4.4 Effect of wheel speed on specific EDDG energy (Pulse current = 7 A; pulse on-time = 100  $\mu$ s; duty factor = 0.64; voltage = 40 V).
- 4.5 Effect of pulse on-time on cutting force and temperature (Pulse current = 7 A; wheel speed = 2.5 m/s; duty factor = 0.64; voltage = 40 V).
- 4.6 Effect of pulse on-time on sp. EDDG energy (Pulse current = 7 A; wheel speed = 2.5 m/s; duty factor = 0.64; voltage = 40 V).
- 4.7 Effect of duty factor on cutting force and temperature (Current = 5 A; wheel speed = 5 m/s; pulse on-time = 100  $\mu$ s; voltage = 40 V).
- 4.8 Effect of duty factor on specific EDDG energy (Current = 5 A; Wheel speed = 5 m/s; Pulse on-time = 100  $\mu$ s; voltage = 40 V).

- 
- 4.9 Specific energy in EDDG and EDM with rotating disc (Disc speed = 2.5 *m/s*; pulse on-time = 100  $\mu$ s; duty factor = 0.64; voltage = 40 *V*).
- 4.10 Specific energy in EDDG and EDM with rotating disc (Pulse current = 7 A; disc speed = 2.5 *m/s*; duty factor = 0.64; voltage = 40 *V*).
- 4.11 Comparison of EDDG temperature with EDM with rotating disc (Voltage = 40 *V*, pulse on-time = 100  $\mu$ s, duty factor = 0.64 and wheel speed = 2.5 *m/s*).

# List of Tables

- 1.1 Advanced engineering materials
- 1.2 Classification of hybrid machining processes.
- 1.3 Interaction of different machining process to develop hybrid-machining process.
- 2.1 Wheel specification and dressing conditions.
- 2.2 Factors and their levels.
- 2.3 ANOVA table for significance testing of regression model.
- 3.1  $3^3$  full factorial design (Voltage = 40 V and duty factor = 0.64).
- 3.2 ANOVA for temperature regression equation.
- 3.3 ANOVA for MRR regression equation.
- 4.1 Specific energy in various processes.
- B.1 Specific energy in EDDG with varying current (Voltage = 40 V, wheel speed = 2.5 m/s, pulse on-time = 100  $\mu$ s and duty factor = 0.64).
- B.2 Specific energy in EDDG with varying wheel speed (Voltage = 40 V, pulse current = 5 A, pulse on-time = 100  $\mu$ s and duty factor = 0.64).
- B.3 Specific energy in EDDG with varying pulse on-time (Voltage = 40 V, pulse current = 7 A, duty factor = 0.64 and wheel speed = 5 m/s).
- B.4 Specific energy in EDDG with varying duty factor (Voltage = 40 V, pulse current = 5 A, pulse on-time = 100  $\mu$ s and wheel speed = 5 m/s).
- B.5 Specific energy in EDM with rotating disc with varying current (Voltage = 40 V, duty factor = 0.64, pulse on-time = 100  $\mu$ s and wheel speed = 5 m/s).
- B.6 Specific energy in EDM with rotating disc with varying pulse on-time (Voltage = 40 V, duty factor = 0.64, current = 7 A and wheel speed = 5 m/s).

# Nomenclature

---

$a_A$	Plasma radius at anode surface
$a_c$	Plasma radius at cathode surface
ANOVA	Analysis of variance
DoF	Degree of freedom
$e$	Residual
$f$	Number of factors
$F_0$	Value of F-distribution
$F_t$	Tangential (cutting) force
$F_{(\alpha)}$	Critical value of $F$ -distribution at $\alpha$ level if significance
$g_w$	Interelectrode gap width ( $\mu\text{m}$ )
$I$	Pulse current (A)
$I$	Unit matrix
$k$	number of levels of each factor
MRR	Material removal rate
MSR	Mean of squares due to regression
MSE	Mean of squares due to residual errors
$P_D$	Electric discharge power (W)
$P_G$	Grinding power (W)
$P_h$	Abrasive protrusion height ( $\mu\text{m}$ )
$q_A$	Heat flux at anode surface
$q_C$	Heat flux at cathode surface
SSE	Sum of squares due to residual errors
SSR	Sum of squares due to regression
SST	Total sum of squares
$t$	machining time (sec)
$T_{\text{on}}$	Pulse on-time ( $\mu\text{s}$ )
$V$	Voltage (V)
$V_b$	Breakdown voltage (V)

---

$x$	Independent variables (factors)
$y$	Dependent variables (responses)

### Greek Symbols

$\alpha$	Level of significance
$\beta$	Regression coefficients
$\tau$	Duty factor
$\xi$	Vector of errors



# Chapter 1

## Introduction and Literature Review

---

### 1.1 Introduction

Today's era of mass-customization and highly competitive market posed challenge before rapidly evolving field of science and technology. Particularly, in the area of material sciences in terms of materials developed for superior performances. Such materials popularly known as *Advanced engineering materials* and may be defined as “the materials having greatly improved thermal, chemical and mechanical properties such as improved strength, heat resistance, wear resistance, and corrosion resistance” [1] viz. titanium and its alloy, cemented carbides, polycrystalline diamonds (PCD), metal matrix composites, etc.

The following table gives an overview of some of the advanced engineering materials.

Materials	Special Characteristics	Applications
Cemented carbides	High wear resistance	Metal forming dies, cutting tools.
Polycrystalline Diamond (PCD)	High strength and high toughness	Cutting tools, rock-drilling bits, wiredrawing dies.
Titanium and its alloys	High strength to weight ratio and excellent corrosion resistance [2]	Used in airframes and engine components in aerospace industry.
Ceramic materials (Aluminum oxide, zirconium oxide, titanium oxide, silicon nitride etc)[3]	High flexural strength, low density, high hardness and brittleness, high compressive strength at high temperatures.	Gas turbines, rocket engines, melting crucibles
Particle Reinforced Metal Matrix Composites (PRMMC) [4]	hardness, strength and resistance of the reinforcement are combined with the ductility and toughness of a matrix material	automotive and aerospace industries (Silicon carbide particle reinforced aluminium MMC)

Table 1.1 Advanced engineering materials

Obvious fallout of such advanced engineering materials is difficulty in shaping them. Limitations of conventional machining methods in shaping of these advanced difficult-to-machine materials due to their improved mechanical properties opened a door to unconventional machining methods to step in. Unconventional machining processes are defined as recently developed process (developed after WW II) that apply machining principles based on physical or chemical phenomenon that differ substantially from those applied in traditional machining. The difference mainly lies in the application of innovative energy sources (LASER, plasma torch, ultrasonic vibrations, etc.) and truly the process is much more driven by chemical and physical phenomena like etching, thermofusion, and cavitation rather than by mechanical forces.

But, as pointed out by Pandey [5],

- i. Unconventional methods cannot replace the conventional machining processes and
- ii. A particular machining method found suitable under the given conditions might not be equally efficient under the other conditions.

Above remarks underline the need of mutual assistance between conventional and unconventional machining processes, can be exploited to tackle the problems created in machining of advanced engineering materials. This mutual assisted process is known as *hybrid machining process*. The process under investigation in the present thesis is Electrodischarge Diamond Grinding (EDDG).

## 1.2 Electrodischarge Diamond Grinding (EDDG)

Electrodischarge diamond grinding is a *hybrid machining process* in which a metal bonded diamond wheel is used and simultaneously it acts as an electrode for electrodischarge action. Mechanical abrasion is combined with the electro-erosion of electrodischarge machining. In EDDG, mechanical abrasion is introduced in the EDG process when an electrically conductive abrasive wheel is used (instead of a non-abrasive graphite wheel) with a proper coolant, which also acts as a dielectric medium for electrodischarge machining. Adjusting wheel speeds and electrodischarge pulse parameters can control the mechanical grinding and electrodischarge erosion.

There are two basic configurations by which the combination of grinding and electrodischarge machining is accomplished. In the first one, workpiece itself acts as a

dressing electrode whereby both the grinding and wheel dressing zones are combined. The work material is thus subjected to both the actions of diamond grains and electrical discharges simultaneously which cause abrasion and material softening/removal, respectively. The reduction of grinding forces and power due to spark induced thermal softening of the work, and enhanced wheel performance due to continuous in-process dressing and declogging of wheel are salient features of this process. Though the construction is simple, this arrangement precludes independent optimization of grinding and dressing operation, which in some cases might result in wasteful diamond wear. In the second configuration, a separate electrode accomplishes electrodischarge dressing of the wheel outside the grinding zone. The discharges are utilized for the renewal of the wheel topography alone and do not exert any influence on the removal of material from work. The wheel, however, can be dressed as and when the need arises, at an optimum rate, irrespective of the grinding conditions.

The process under investigation in present thesis uses the principle described in mode 1 above (Fig. 1.1a). The first configuration of the process has been employed for surface grinding and face grinding mode are as shown in Fig.1.2 and Fig.1.3, respectively. ' $P_h$ ' denotes protrusion height of abrasive grains of grinding wheel. For a particular voltage applied across metal bonded wheel, there is a critical gap required for spark to occur ( $g$ ). For any gap value greater than ' $g$ ', no sparking would be possible. So, sparking in grinding zone serves two-fold purpose. One, it removes some amount of material by EDM action improving material removal rate of the

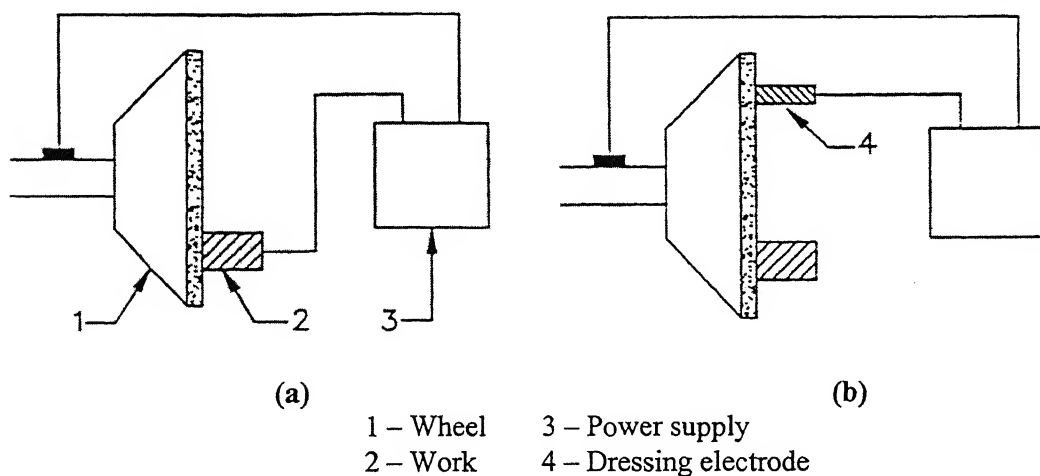


**Fig. 1.1 Basic configurations of EDM-grinding hybrid processes (a) Combined dressing and grinding zones, (b) Isolated dressing and grinding zones.**

EDDG process, and secondly, it thermally softens the work material so that less force is required for the following abrasive action during machining.

The EDDG term often causes confusion with another process in EDM category named as “Electrical Discharge Grinding” (EDG). In EDG, a rotating electrically conducting wheel is used as the electrode [6]. But importantly, there is no physical contact between wheel and the workpiece to be machined whereas, in EDDG, EDM action occurs between metallic bond material of the wheel and the workpiece. Simultaneously, abrasive grains get engaged in removing material by abrasion like conventional grinding. In the true sense, EDG can be better named as “EDM with rotating disk electrode” [7].

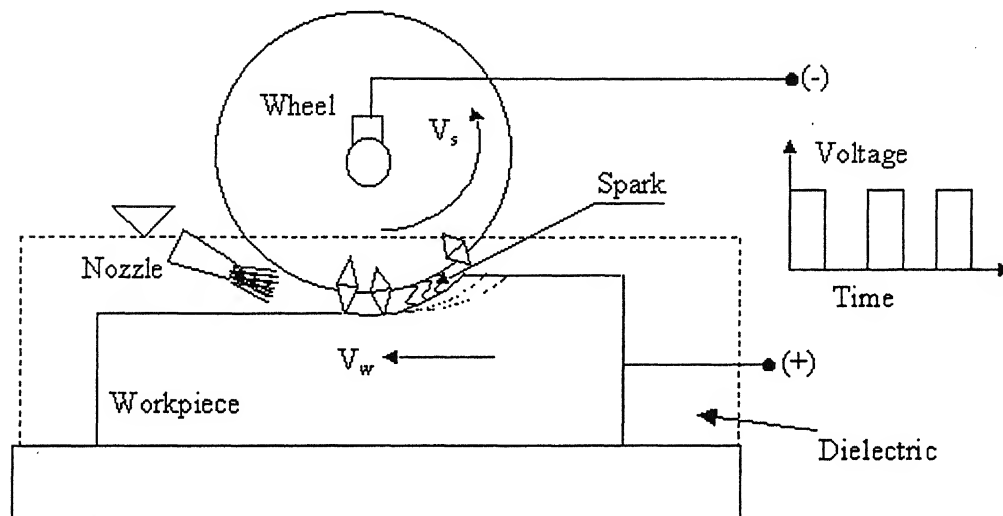


**Fig. 1.2 EDDG in surface grinding mode**

The improved grinding performance in EDDG is due to continuous in process dressing and declogging of the grinding wheel. Consequently, the grinding wheel can maintain its grinding ability without becoming dull. Since the contributions of mechanical abrasion and thermal erosion to process performances are adjustable, the EDDG can be used either in a grinding dominant state with a relatively less effect of electrical discharge to acquire a reduced heat-affected surface layer, or in an EDM dominant state with a relatively less effect of grinding to reduce machining force, or in a well balanced state between the grinding and EDM. Applications of this process include machining of components made of advanced engineering materials such as

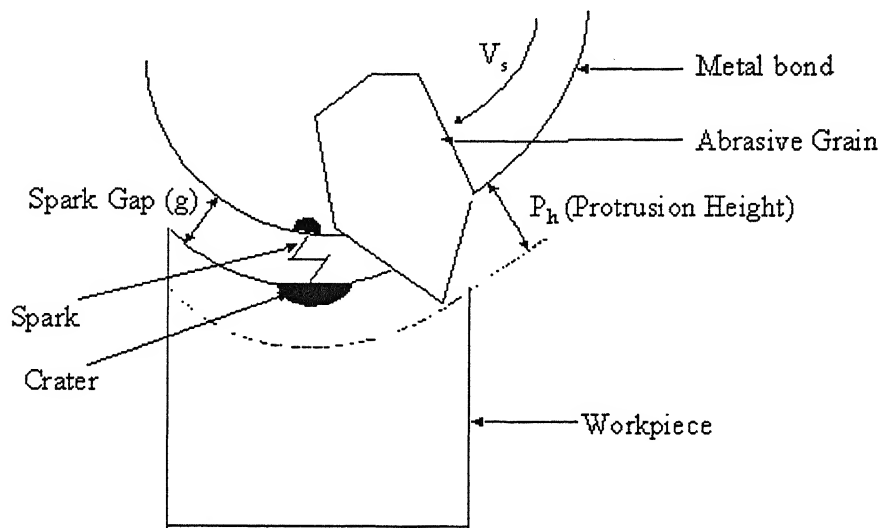


**Fig. 1.3 EDDG in face grinding mode**

Al-SiC composites (duralcan), inconel, titanium alloy, tungsten carbide, high speed steel (HSS), cemented carbide, polycrystalline diamond, etc.

### 1.3 Literature Survey

Electro-discharge diamonds grinding is a comparatively newer process. To understand the mechanism of the process, study of its constituent process, i.e. electro discharge machining (EDM) and grinding is essential. Following section gives review of literature concerned.

#### 1.3.1 Electrodischarge machining and grinding

EDM is an inefficient process. Thermal modeling of the process has indicated that the fraction of the molten material, which is physically not removed but redeposited on the parent material surface, could be as high as 80% [8]. The recast layer and the heat-affected material contain numerous microcracks, which degrade the fatigue strength of the material. Pandey et al [9] proposed a model for calculating thickness of the heat affected zone (HAZ) due to a single spark.

EDM of composite materials containing electrically nonconducting phases possess a few problems. The non-conducting material particles hamper the process stability and impede the material removal resulting in very low stock removal rates. More serious problem is associated with die sinking of such materials. As machining progresses, due to inhomogeneity of the work material, if by chance a localized layer

of insulating material surfaces up, the control system of the machine tool would misinterpret the situation as an open circuit. This would lead to a continuous feed motion being imparted to the electrode and consequent collision and damage of both the tool and workpiece.

In connection with use of experimental designs for the investigations concerned with EDM, Scott et al [10] used orthogonal array ( $L_{18}$ ) for analyzing the material removal rate (MRR) and surface finish (SF) in wire EDM. Further, mathematical models developed from matrix experiments used for optimization of conflicting responses i.e. MRR and SF. Rajurkar et al [11] did multi-objective optimization of EDM with orbital motion of tool electrode. Here also fractional factorial ( $L_{27}$ ) design was employed to predict the performance (MRR and SF). Matrix models were chosen on the assumption that the effect of interactions among the factors is negligible.

No literature was available in which experimental investigation of temperature measurement of workpiece in EDM had been done. Obara et al [12] tried to find average wire temperature distribution in wire EDM. They developed an electronic circuit and from discharging currents and voltages average temperature was found. A maximum wire temperature obtained in this analysis was about 100°C. Abbinski et al [13] have reported experimental difficulties in measurement of plasma channel temperature like short discharge duration, very small interelectrode gap and the influence of dielectric fluid. Plasma temperature was determined from the relative intensity of spectral lines of FeI. Two photomultipliers were used to register light emitted by the whole plasma volume.

In case of conventional machining processes, machining of any materials is possible only with tool made of material harder than workpiece. Hardness of advanced engineering material is comparable with diamond, hardest known abrasive. Grinding of hard and brittle materials is characterized by high normal forces because of indentation of abrasive grains into workpiece becomes difficult. [14]. It results in elastic deformation in grinding wheel and subsequent fallout in loss of accuracy. Also, problems associated with grinding wheels are glazing of the wheel as well as loading of the wheels.

As far as temperature measurement in conventional grinding is concerned, Shaw [15] utilized property of tool-work interface to act as a thermocouple. This is

useful in finding out surface temperatures in grinding which would be otherwise very difficult to measure. In the configuration shown in fig. 1.1, tool-work interface constitutes the hot junction of a thermocouple circuit. It was mentioned that silicon carbide-steel combination has very much higher thermoelectric power than that for ordinary metal combination. But, the impedance of the grinding wheel compared with that of ordinary metals makes it difficult to obtain accurate values.

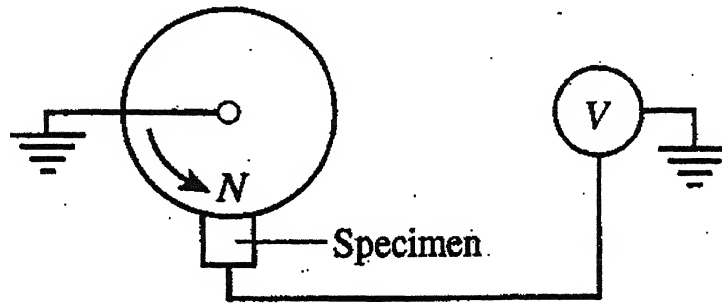


Fig. 1.4 A grit-chip thermocouple circuit [15]

Subsurface temperature measurement can be done using buried thermocouple technique in which a micro hole is drilled from bottom side of the work to accommodate thermocouple wire. This technique is useful in studying subsurface phenomena such as over-tempering, rehardening and burn. But, estimation of temperatures at grit-work interface is very difficult. Extrapolation gives inaccurate results because of very steep temperature gradients at the surface.

Advanced methods like use of infrared radiation pyrometer and physically vapor deposition (PVD) are reported in references [16,17]. Infrared pyrometry is based on the principle that the heated material emits infrared flux whose intensity depends upon temperature of material. Ueda et al [16] proposed use of optical fibers to catch the flux. They measured the temperature of cutting grains on wheel surface. Another novel method is use of PVD. A single material with a specific melting point is vapor deposited on the polished surface of workpiece. A pair of specimen are fastened together and used for grinding. After grinding by analyzing the film nature (melted zone and unmelted zone) temperature distribution can be found out.

### 1.3.2 Hybrid Machining Processes

One of the effective methods to achieve high performance indices for machining consists in combining usually two (say, physical, and chemical processes acting on workpiece material) into one machining process, which is often termed as “hybrid machining process”. [18] These processes are developed to exploit the potential advantages and to restrict the disadvantages associated with an individual constituent process. Usually, the performance of hybrid process is better than the sum of their individual performance with the same parameter settings.

Electrochemical grinding (ECG) has found applications in manufacture of carbide cutting tools, creep resisting alloys (e.g. Inconel, Nimonic), titanium alloys, metal matrix composites. This hybrid process is a combination of ECM and fine grinding for the machining of hard or fragile electrically conductive materials. [6]. Electrochemical grinding with metal bonded abrasive tool (AECG), consists in combination of mechanical and electrochemical processes, acting on the workpiece, that considerably changes performance indexes of the machining process. Process productivity and surface layer properties are reported to be improved while tool wear and energy consumption decreases. [8]. Typically, 90% of the material removal is by electrochemical means and the rest by abrasion

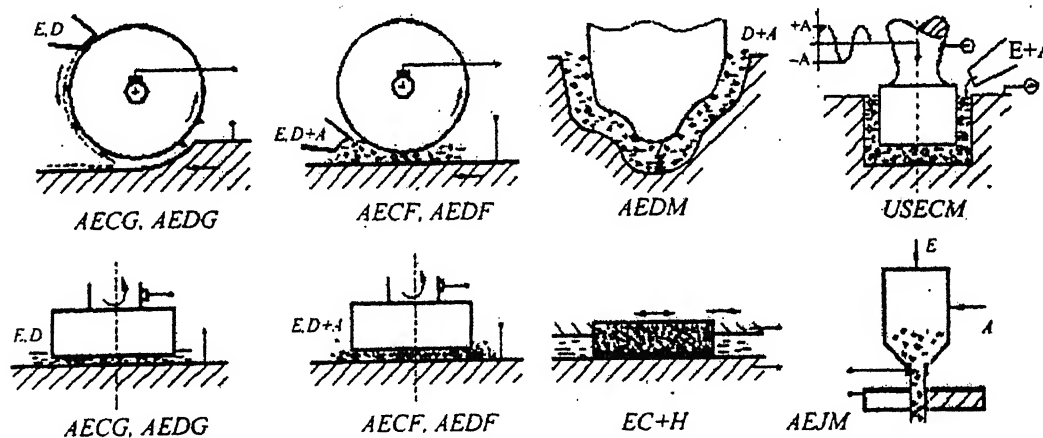
Process	Combination of Energy Sources	Mechanism of Material Removal	Tool	Transfer Media
ECSM /ECAM	Thermal and Electrochemical	Melting and Evaporation	Electrode	Electrolyte
EDAG	Thermal and Mechanical	Melting, Evaporation and abrasion	Metal bonded abrasive wheel	Dielectric
ECAG	Electrochemical and Mechanical	Electrochemical dissolution and abrasion	Metal bonded abrasive wheel	Electrolyte
LAE	Thermal and chemical	Chemical dissolution and heating	Mask	Etchant
LAECM	Thermal and Electrochemical	Electrochemical dissolution and heating	Electrode	Electrolyte
LAT/PAT	Thermal and Mechanical	Shearing and Heating	Turning tool	Air



UAEDM	Thermal and Ultrasonic Vibration	Melting & Evaporation	Sonotrode	Dielectric
UAECM	Electrochemical and Ultrasonic Vibration	Electrochemical dissolution	Sonotrode	Electrolyte
UALBM	Thermal and Ultrasonic Vibration	Melting & Evaporation	Laser beam	Air
UAG	Abrasion and Ultrasonic Vibration	Abrasion	Sonotrode of abrasive wheel	Coolant
UAT	Ultrasonic Vibration and Mechanical	Shearing	Turning tool	Air
BEDMM	Thermal, Mechanical & Electrochemical	Electrochemical, Melting and Mechanical Rupture	Rotating Metal brush	Water glass solution in water

**Table 1.2 Classification of hybrid machining processes [19]**

Another hybrid process related to ECM is Electrochemical discharge machining (ECDM). In this process, the discharge between the cathode and electrolyte occurring mainly due to electrolytic gas generation at the surface tool (cathode) electrode is employed for removal of material. ECDM appears to have potential for machining of materials having low machinability, high strength and importantly, electrically conducting and as well as non-conducting materials like composites. ECDM process has applications in micro welding. But, ECDM has very limited acceptance because of its limited capacity and complicated phenomena associated with it [20].



A: abrasive; D: dielectric; E: electrolyte

**Fig 1.5 Selected methods of abrasive electrical machining [18]**

Table 1.3 Interaction of different machining process to develop hybrid-machining process

			Thermal Processes				Chemical and Electro-chemical Processes		Mechanical Processes			
Thermal Processes	EDM		EDM	LBM	EBM	PBM	CHM	ECM	ABRASION (A)	USM	FLOW (F)	CUTTING (C)
	EDM		EDM					ECM	EDAG	UAEDM		
	LBM			LBM			LAE	LAECM		UALBM		LAT
	EBM				EBM							
	PBM					PBM						PAT
Chemical and Electro-chemical Processes	CHM			EALBM			CHM	ECM	EBM		CHP	
	ECM		ECM	LAECM					ECAG/ECAM	UAECM		
Mechanical Processes	ABRASION(A)		EDAG				EEM	ECAG	AM	UAG		
	USM		UAEDM	UALBM				UAECM	UAG	USM	UAP	UAT
	FLUID FLOW (F)						CHP			UAP	FFM	
	CUTTING(C)			LAT		PAT				UAT		CUTTING

- AM: Abrasive Machining
- CHM/ CHP: Chemical Machining/ Chemical Polishing
- EALBM: Etching Assisted Laser Beam Machining
- EBM: Electron Beam Machining
- ECAG/ECAM: Electro-Chemical Abrasive Grinding/ Electro-Chemical Abrasive Honing
- ECM/ECAM: Electro-chemical Discharge /Arc Machining
- ECM: Electro- Chemical Machining
- EDAG: Electro- Discharge Abrasive Grinding
- EDM: Electrical Discharge Machining
- EEM: Elastic Emission Machining
- FFM: Fluid Flow Machining
- LAE: Laser Assisted Etching
- LAECM: Laser Assisted Electro- chemical Machining
- LAT: Laser Assisted Turning
- LBM: Laser Beam Machining
- PAT: Plasma Assisted Turning
- PBM: Plasma Beam Machining
- UAECM: Ultrasonic Assisted Electro- chemical Machining
- UAEDM: Ultrasonic Assisted Electrical Discharge Machining
- UAG: Ultrasonic Assisted Grinding
- UALBM: Ultrasonic Assisted Laser Beam Machining
- UAP: Ultrasonic Assisted Polishing
- UAT: Ultrasonic Assisted Turning

Main obstacle in machining any material by conventional method is difference between workpiece and tool hardness. So, efforts were made to explore the means to soften the workpiece material before it actually gets machined by conventional tools. Hot machining finding its way in this direction. Kitagawa et al [21] proposed plasma hot machining. In this method, workpiece temperature is increased by plasma arcs and then machined by turning. This process is proved to be uneconomical in cases where hardness is directly proportional to the temperature upto a certain limit, the case which occurs with Alumina.

Ultrasonic machining (USM) and EDM are both characterized by their ability of machining hard and brittle materials. The main disadvantage of each process lies in its comparatively low material removal rate. Koshimuzu et al [22] had investigated effect of combination of USM with EDM in machining of tungsten carbide. In combined machining, it was considered that the tungsten carbide, which is weakened by the heat of electrical discharges, was efficiently removed through the hammering effect of the abrasive grains. Material removal rate was found to be increased by 50-80% comparing with USM.

### 1.3.3 Electrodischarge Diamond Grinding (EDDG):

EDDG being new process, literature available is scarce. It also indicates there is lot of room for research in this process. In previous section, hybrid machining processes are reviewed in the context of machining of advanced engineering materials.

Wheel loading is matter of concern in conventional grinding of advanced materials. To avoid frequent dressing of wheels on-line dressing is could be a best remedy. As discussed in earlier section electrochemical grinding (ECG) attempts such on-line dressing. But, electrical activation of the diamond grinding wheel surface in ECG is not normally subject to control. This can be attributed to electroerosive processes that that accompany the anodic dissolution of metal are of random nature. [23]. Also some of hybrid machining process discussed above like ECG, ECSM uses electrolyte as a working fluid. Presence of the ions in the medium would induce arcs, which would damage work. Use of electrolytes or coolants with ions causes increase in material removal rates. However, when precision finishing is pursued for materials with heterogeneous phases such as conductive ceramics, metal matrix composites and

superalloys, the use of dielectric medium is essential not only to avoid arcing, but also to avoid detrimental stray current attacking, selective dissolution among the heterogeneous phases, and grain boundary erosion caused by uncontrollable electrolysis effects. Feasibility of the EDDG can be seen against these drawbacks of the hybrid processes for machining of advanced engineering materials.

Bakhtiarov [24] analyzed efficiency of diamond wheels after contact erosion dressing. Efficiency of metallic bonded diamond wheels after contact-erosion dressing was compared with the efficiency of the same wheels after traditional abrasive dressing. It was found that specific diamond usage was slightly greater than after abrasive dressing because of the increased height of projection of the grains above the level of the bond. However, wheel life in terms of the period between dressings is 5-10 times greater after contact-erosion dressing than after abrasive dressing. Also, cutting property of the wheel (i.e. volume of material removed per unit force per unit time) dressed by this method is more that double the value for the wheels after abrasive dressing. This is because after contact erosion dressing the height of the diamond grains projecting above the bond is equivalent 30-60% of the total grain size, whereas after abrasive dressing it is 5-10%.

Ayoma and Inasaki [25] studied the effect of combination of conventional grinding and EDM on the machining force, the wear of the grinding wheel, the geometrical accuracy, and the surface roughness of the workpiece experimentally. Materials used were cemented carbides, advanced ceramics, and sendust (it has excellent magnetic properties). Cutting forces were found to be reduced. This reduction further causes improved straightness of the groove. However, side face of the groove becomes larger. The main disadvantage reported is high wear rate of the wheel. They proposed to use wheel with metal bond having tungsten since tungsten alloy is a good resistant to the high temperature generated by the electrical discharges.

Rajurkar et al [26] introduced an Abrasive Electrodischarge grinding (AEDG) monitoring and control system. Also, experiments were conducted on advanced materials like Al-SiC composite (Duralcan) and titanium alloy (Ti-6Al-4V). Process responses like material removal rate (MRR) and surface finish of AEDG were compared with that of EDM and EDG. Improvement in MRR and surface finish was observed with AEDG compared to the other processes for the above stated advanced materials. Monitoring and control system comprises of a dynamometer for

measurement of forces and a electrodischarge monitor for detecting the status of electrical discharges within the inter electrode gap (IEG) such as normal spark, arc or short-circuit. A computer based data acquisition system, capable of measuring force signals and discharge signals, has the capability of monitoring both the grinding and electrodischarge processes.

Koshy [27] has given experimental and theoretical work into EDDG. The accent in the experimental work is on examining the role of electrical spark/discharge at the wheel-work interface in enhancing grinding performance. Mechanism of material removal was proposed for high speed steel (HSS) and cemented carbide as work material. Effects of current on material removal rate as well as radial wear of wheel were examined. It has been found that increase in current leads to improvement in material removal rate and also increased wheel wear rate. Effect on normal as well as tangential forces were also analyzed. Decrease in force components was observed. This is due to thermal softening of the work by electrical discharges. Diamond wheel topography modeling was also done. Information on the topography of diamond wheels is pre requisite for modeling of EDDG.

Gupta et al [28] did experimental work on EDDG using HSS as work material. Experiments were conducted to find the effect of current, voltage, and pulse on-time and duty factor on material removal rate and grinding forces. Observations indicate that normal grinding force decreases with increase in current; this trend reverses with increase in pulse on-time. Material removal rate was found to be increased with increasing current and pulse on-time, while the same decreases with increasing voltage and duty factor.

Yadava [19] presented Finite Element Analysis of EDDG. Temperature distribution models were developed separately for cut-off grinding and EDM. By using principle of superposition, temperature distribution model for EDDG was proposed. Using this temperature distribution model, thermal stresses were predicted. Effects of process parameters (current, pulse on-time, duty cycle) on temperature distribution and thermal stresses in the workpiece were studied. It has been found that higher duty cycle with given off-time gives higher temperature, because increase in current leads to increase in peak temperature due to increase in heat flux. The temperature gradient along the depth is found to be steeper than the temperature gradient along its radial distance from the center of the spark. It is also noted that

temperature gradient is very high upto 0.63 mm depth from top surface for all currents. Beyond this depth, temperature gradient variation is almost zero. Hence, from thermal stresses point of view, this thin surface layer is most critical. After this depth, temperature gradient gradually decreases. Almost no change in temperature at the top surface as well as along the depth is observed beyond the assumed spark radius.

From the review of the literature, following points can be mentioned:

- Most of the experimental work done in EDDG is of exploratory in nature.
- In case of EDM, no literature was found on experimental investigation into temperature of workpiece.
- Scientific methods like Design of Experiments (DOE) have not been employed for experimentation in EDDG.
- Specific energy during EDDG process has not been investigated.

## **1.4 Scope and Organization of the thesis:**

### **1.4.1 Objectives of the thesis**

From, literature survey presented above scope of the present work is defined. EDDG being new process, most of the work done is exploratory in nature. Process investigations using scientific tools like experimental design have not been done.

Following are the objectives of the work.

- To study the effect of process parameters on the material removal rate using design of experiments and to develop a regression model for it.
- To study the effect of process parameters on the average temperature in the workpiece by the use of experimental design, and also to develop a regression model for it.
- To study the effect of the process parameters on the specific energy of the EDDG and comparison with EDM.

### **1.4.2 Organization of the thesis**

Present thesis work is about experimental investigation of Electrodischarge Diamond Grinding (EDDG).

**Chapter 1** provides overview of advanced engineering materials and gives significance of hybrid processes in general and EDDG in particular. Also, a brief introduction of EDDG is given. It also comprises of literature review related to the work done in the EDDG process is presented and up to some extent its constituent processes like EDM and conventional grinding. Glimpses of various temperature measurement techniques are also provided. Chapter ends with mentioning scope of the work and its organization of the thesis.

**Chapter 2** is about experimentation. It explains techniques used for temperature measurement and force measurement. Precautions taken during experimentation like wheel truing, dressing, etc. are also discussed. A brief theory of Design of Experiments methodology and model fitting using regression with its significance checking is given.

**Chapter 3** analyses the results of temperature measurement and material removal rate using experimental design. Regression model and its significance are tested using analysis of variance. Effects of process parameters like current, pulse on-time and wheel speed are presented.

**Chapter 4** discusses specific energy in EDDG. Details of experiments done for calculating specific energy in EDDG are provided. Also, variation of specific energy with various process parameters is also investigated. A comparison of EDDG is also done with EDM process with reference to specific energy.

Conclusions constitute **Chapter 6**. It highlights scope for the future work also.

## Experimentation

## 2.1 Experimental set-up

All the experiments are conducted on EDM machine. Machine used was ELEKTRA EDM (ZNC). It has numerical control in Z-axis. A special grinding attachment, developed by Koshy [27], is used for the present experimentation.

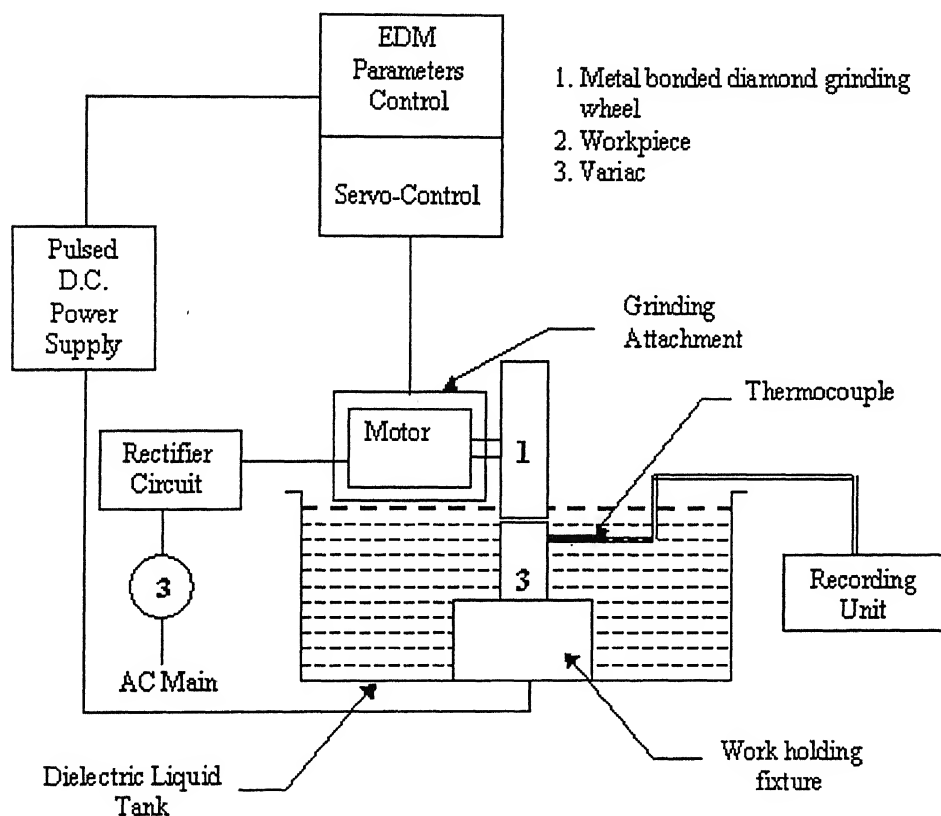


**Fig. 2.1 General scheme of Electrodischarge Diamond Grinding**

The grinding attachment can be mounted on Z-axis (EDM electrode). A metal bonded grinding wheel acts, as an electrode required for EDM action.

The grinding attachment is mounted on the ram of EDM machine to rotate the metal bonded diamond wheel about its axis parallel to the machining table. Rotational speed of the grinding wheel is controlled by varying input voltage (using variac) of



the motor that drives the wheel. While machining, the entire attachment with ram is fed downward under the servomechanism of the EDM machine. Physical contact between metallic bond and workpiece is avoided by gap sensing mechanism of the servo system. Gap between bond and workpiece is defined by servo reference voltage setting.

Since the machine has Z-axis numerical control to facilitate EDM action, plunge mode of grinding is employed. Basically in plunge mode of grinding depending upon wheel thickness and workpiece thickness, 2 types can be distinguished. [15]

1. Cut-off grinding
2. Face grinding

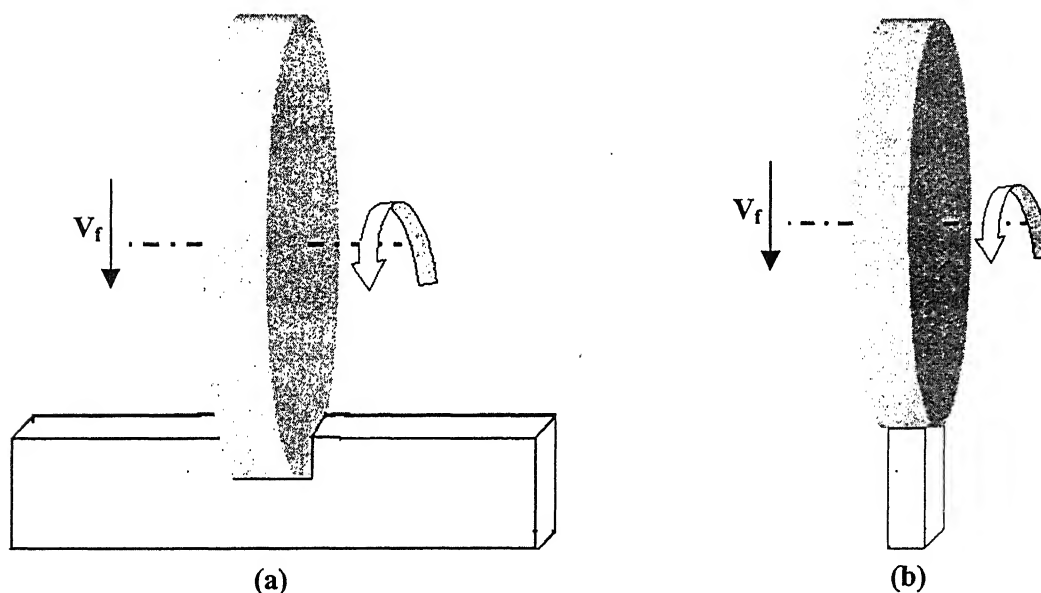


**Fig. 2.2 Different modes of plunge grinding (a) Cut-off grinding (b) Face grinding**

## 2.2 Wheel Truing and Dressing

In surface grinding with cross feed, each table stroke or workpiece revolution results in a wheel wear profile as shown in Fig. 2.3. This is due to the initial rapid breakdown of the wheel leading edge and then progressive distribution of the workload over the wheel width as further breakdown occurs. Once a stable condition is reached when the grits can withstand the imposed workload, the initial dressed wheel condition is not found to affect the wheel characteristics significantly. But in case of form/plunge grinding, workload is evenly distributed over the wheel width.

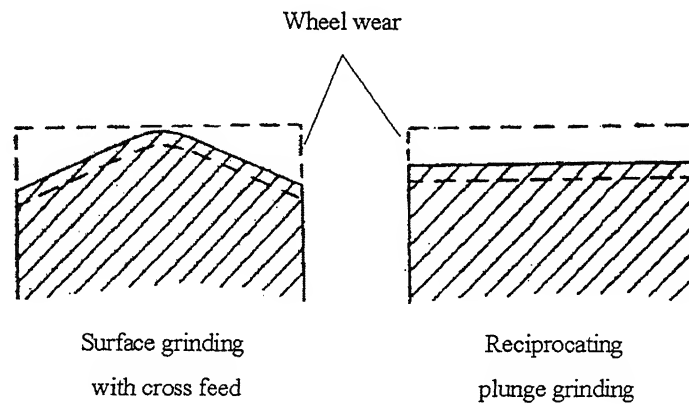


**Fig. 2.3 Wheel wear in grinding [29]**

The workload per grit is, therefore, dependent on the machine parameters and the wheel composition. As shown in **Fig.2.3**, the wheel wear is same over the working width. When grinding under these conditions, the wheel performance is found to be significantly affected by dressing procedure. Present study is based on plunge mode of grinding.

In the present work, face-grinding mode (**Fig 2.2b**) is employed. Coarse machining of the wheel is termed as ‘truing’ and is required to eliminate wheel ‘out of roundness’, and less severe ‘machining’ is termed as ‘dressing’ which prepares the wheel surface for grinding. For electrodischarge action, working gap across wheel and workpiece is critical. To maintain this gap constant during wheel rotations, circularity of the wheel is an important consideration.

Taking into account above discussed factors, following procedure was employed for truing and dressing.

The diamond wheel was initially trued with a silicon carbide wheel run in mesh with it. Truing is accomplished by abrasion of the bond by the debris generated at the interface of the two wheels. The slip between the grinding and truing wheels, necessary for truing action, was obtained by orienting their axes such that their peripheral velocities are not collinear along the line of contact. Out of roundness of the wheel is checked with a dial-gauge. Truing operation was continued until radial run-out was reduced to less than  $10\mu m$ .

Thus trued grinding wheel has dimensional accuracy but it cannot be used for experimentation unless properly dressed. Dressing was accomplished by electric discharge action. **Ref.30** gives details of the effect of discharge action on the resultant

wheel topography. At high discharge energy conditions, sufficient grit protrusion is obtained but at the expense of dislodging some abrasive grains. Arriving at the appropriate level of discharge energy entails a compromise between these two conflicting factors. Wheel dressing was done before each experiment so that standard wheel topography could be maintained.

Choice of electrode (work) material for electrodischarge dressing of diamond wheels is a vital consideration. Affinity of diamond for metals has been discussed in Ref. 31. Graphitization of diamond is remarkable when heated with *Fe*. Lower affinity of diamond was observed with soft metals viz. *Al*, *Cu*. Therefore, *Cu* was chosen for dressing of diamond wheels. Table 2.1 gives process parameters for wheel dressing.

---

Wheel Specifications		Wheel Dressing Conditions	
Abrasive	Diamond	Voltage	60 V
Diameter	100 mm	Current	10 A
Bore	33 H7	Pulse on-time	100 $\mu$ s
Thickness	7 mm	Duty factor	0.48
Impregnation	3 mm	Wheel speed	1 m/s
Concentration	75%	Duration	2 min
Grit size	80/100		
Bond material	Bronze		

---

**Table 2.1 Wheel specification and dressing conditions**

### 2.3 Design of Experiments (DOE)

Literally, an experiment is a *test*. A *designed experiment* is a test or series of tests in which purposeful changes are made to the input variables of a process or system so that we may observe and identify the reasons for changes in output response [32].

DOE is an analytical tool that helps reveal the critical parameters of a manufacturing process without requiring that every possible combination of process factors be investigated. For any process under study, it is required for investigator to

decide which are responses and which are factors. It is an active method of obtaining information as opposed to passive observations (like statistical control charts).

In terminology of experimental design, a treatment is a certain combination of factor levels, which affect the response variables of interest. DOE is used to determine the impact of factors on the response variables. With quantitative factors, which vary on a continuous scale, we may obtain information of the variable's behavior even for factor levels that have not been experimentally determined. Assuming that the behavior of the response variable is representative of the process, a quantitative model (of multiple regression type) may be developed to depict its relationship with the control factors of interest.

EDDG being hybrid-machining process, it comprises of large number of factors as listed below.

*EDM parameters*

1. Pulse current
2. Discharge voltage
3. Pulse on-time
4. Duty factor
5. Dielectric media.
6. Polarity

*Grinding Parameters*

1. Cutting speed
2. Wheel size
3. Concentration

*Workpiece*

1. Material
2. Workpiece size

Responses:

1. Temperature of the workpiece
2. Material Removal Rate.

Experiments were performed for HSS workpiece with same kind of grinding wheel with EDM-30 oil as a dielectric liquid. Also, keeping in view that process being hybrid and under development stage, to get full idea about interactions (**Fig.2.4**)

among factors it was decided to use full factorial design. Number of experiments to be performed using full factorial design can be given by formula:

$$n = f^k$$

where,  $n$  = Number of experiments

$f$  = Number of factors

$k$  = Number of levels of each factor

For experimentation following factors were decided to study:

1. Pulse current
2. Pulse on-time
3. Cutting speed

So, number of experiments needed to be performed =  $3^3 = 27$

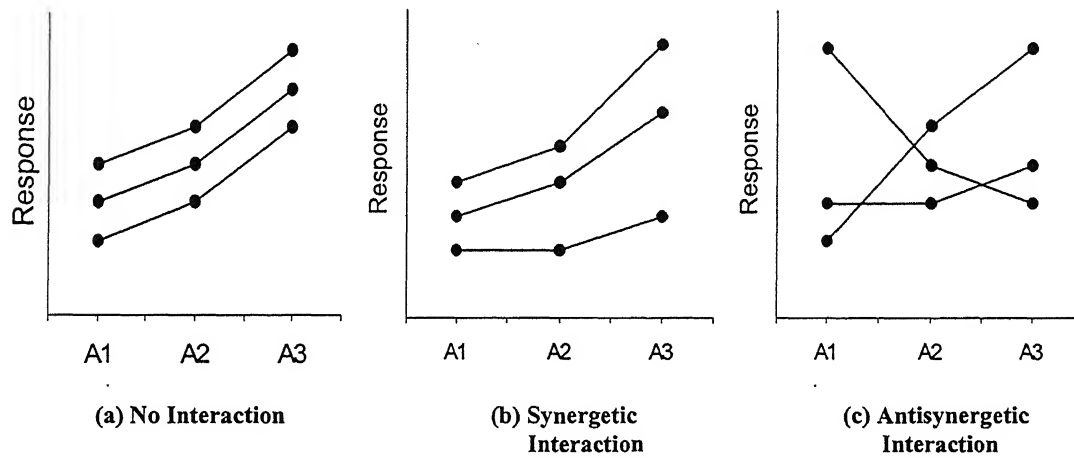


Fig. 2.4 Types of factor interactions

Each factor at 3 levels.

Control Factors	Level I	Level II	Level III	Units
Pulse Current	7	13	19	A
Cutting Speed	2.5	5	7.5	m/s
Pulse on-time	100	200	300	$\mu$ sec

Table 2.2 Factors and their levels

Full factorial plan is as given in Table 3.1. Using such plan a multiple regression model can be fitted into obtained observations. Also, using analysis of

variance (ANOVA) significance of the fitted model can be tested. The theory of model fitting and checking of significance is presented below.

### 2.3.1 Model Fitting [33]

Let  $y$  be dependent variable and we have  $k$  independent variables. The functional relationship can be approximated by

$$y_j = \beta_0 + \beta_1 x_{1j} + \beta_2 x_{2j} + \dots + \beta_k x_{kj} + \xi_j, \quad j = 1, 2, \dots, n$$

Such a model is called a **multiple regression** model.

In matrix notation,

$$y = X\beta + \xi$$

where  $y$  is the  $n$ -dimensional vector of the observations,  $\xi$  is the corresponding vector of errors, and  $\beta$  is a vector that consists of the  $k+1$  coefficients,  $\beta_i$ . The matrix  $X$  is called the design matrix. It has  $n$  rows, one for each data point.

$$X = \begin{pmatrix} 1 & x_{11} & x_{21} & \dots & x_{k1} \\ 1 & x_{12} & x_{22} & \dots & x_{k2} \\ \vdots & \vdots & \vdots & \ddots & \vdots \\ 1 & x_{1n} & x_{2n} & \dots & x_{kn} \end{pmatrix}, \quad \beta = \begin{pmatrix} \beta_0 \\ \beta_1 \\ \vdots \\ \beta_k \end{pmatrix}, \quad y = \begin{pmatrix} y_1 \\ y_2 \\ \vdots \\ y_k \end{pmatrix}, \quad \text{and} \quad \xi = \begin{pmatrix} \xi_1 \\ \xi_2 \\ \vdots \\ \xi_n \end{pmatrix}$$

The least-squares estimate of the vector  $\beta$  is known to be

$$\hat{\beta} = \begin{pmatrix} \hat{\beta}_0 \\ \hat{\beta}_1 \\ \vdots \\ \hat{\beta}_k \end{pmatrix} = (X'X)^{-1} X' y$$

and the vector of estimated values of the dependent variable and the vector of the residuals are, respectively,

$$\hat{y} = \begin{pmatrix} \hat{y}_1 \\ \hat{y}_2 \\ \vdots \\ \hat{y}_k \end{pmatrix} = \begin{pmatrix} \hat{\beta}_0 + \hat{\beta}_1 x_{11} + \dots + \hat{\beta}_k x_{k1} \\ \hat{\beta}_0 + \hat{\beta}_1 x_{12} + \dots + \hat{\beta}_k x_{k2} \\ \vdots \\ \hat{\beta}_0 + \hat{\beta}_1 x_{1n} + \dots + \hat{\beta}_k x_{kn} \end{pmatrix} = X\hat{\beta}$$

$$\begin{aligned} \text{Residual, } e = y - \hat{y} &= y - X\hat{\beta} \\ &= y - X(X'X)^{-1}X'y \\ &= (I - X(X'X)^{-1}X')y, \end{aligned}$$

where,  $I$  is the unit matrix.

### 2.3.2 Analysis of Variance [33]

In order to judge whether the regression equation is significant or not in explaining the relationship between dependent and independent variables,  $F$ -test from the analysis of variance (ANOVA) was conducted.

Consider the following:

$$(y_i - \bar{y}) = (y_i - \hat{y}_i) + (\hat{y}_i - \bar{y})$$

On squaring and summing over  $i$

$$\sum (y_i - \bar{y})^2 = \sum (y_i - \hat{y}_i)^2 + \sum (\hat{y}_i - \bar{y})^2$$

In words,

$$\begin{array}{ccccc} \text{Total sum of squares} & = & \text{Sum of squares} & + & \text{Sum of squares} \\ & & \text{due to residual errors} & & \text{due to regression} \\ (SST) & & (SSE) & & (SSR) \end{array}$$

These sums of squares are computed as:

$$SST = \sum (y_i - \bar{y})^2 = \sum y_i^2 - n\bar{y}^2$$

$$SSR = \sum (y_i - \hat{y}_i)^2$$

$$SSE = SST - SSR$$

The ANOVA table is then prepared as:

Table 2.3 ANOVA table for significance testing of regression model.

Source of variation	Sum of squares	Degrees of freedom	Mean square	$F_0$	$F(\alpha)$
Regression	$SST$	$k$	$MSR$	$MSR/MSE$	$F(k, n-k-1, \alpha)$
Residuals	$SSE$	$n-k-1$	$MSE$		
Total	$SST$	$n-1$			

Here,  $MSR$  stands for the mean of squares due to regression, and is obtained by dividing  $SSR$  by the regression degree of freedom.  $MSE$  means the mean of squares due to residual errors, and is obtained by dividing  $SSE$  the residual degrees of freedom.

By the regression theory,

If  $\beta_1 = \beta_2 = \dots = \beta_k = 0$  then,  $MSR/MSE$  follows the  $F(k, n-k-1, \alpha)$  probability distribution. Hence, if the test statistic  $F_0$  is greater than the critical value  $F$  at the  $\alpha$  level of significance, then it can be concluded that the fitted regression equation is significant in explaining the relationship between  $Y$  and independent variables.

## 2.4 Temperature Measurement

Temperature measurement is an important part of scientific experiments, research and development, and industrial processes. The thermocouple provides a simple and efficient means of measuring temperature because it produces a voltage, which is a function of temperature. This voltage can be read using an analog to digital converter (or any voltmeter), and the temperature can be inferred from consulting standard tables.

A thermocouple works because there is voltage drop across dissimilar metals, which are placed in contact. This voltage is a function of temperature. In principle, a thermocouple can be made from almost any two metals. In practice, several thermocouple types have become standard because of desirable qualities such as linearity of the voltage drop as a function of temperature and large voltage to temperature ratio. Some common thermocouple types are designated as  $J$ ,  $K$ ,  $T$ ,  $E$ ,  $S$ ,  $R$ , and  $B$  depending upon temperature range and material used e.g. type  $S$  has platinum and rhodium wire and is accurate over the range  $0-1600^\circ C$  [34]. The

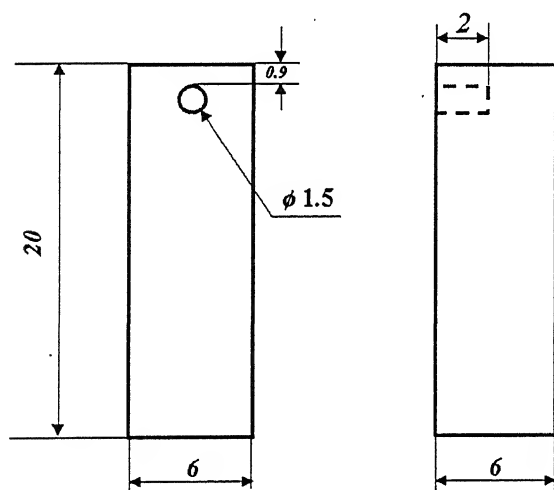


thermocouple leads are joined by welding or soldering. (Thermocouple wires are commonly twisted together, but this is not recommended and can lead to inaccuracies.)

In practice, the industrial thermocouple comprises a sheathed "hot junction" with some form of extension of the two wires (directly or via a connection interface) which terminates at the instrument input; the junction effectively formed at the instrument constitutes the "cold" junction.

Here, *Type K* thermocouple was employed. It is having Chromel-Alumel as thermocouple elements. It has working range from  $-40-1000^{\circ}\text{C}$ . Thermocouple wires are protected with *Inconel* coating having diameter of. 1.5 mm.

A specimen was prepared as shown in fig. 2.5. Small hole of diameter 1.5 mm was drilled using *EDM* since work material is *High Speed Steel* with 10% *cobalt*. Thermocouple wire was then fixed in this hole and thus prepared specimen was used for experimentation.



All dimensions are in mm.  
Material:  
High Speed Steel

**Fig 2.5 Specimen geometry used for experimentation**

A thermocouple tip was placed into the hole. Experiments were conducted in face grinding mode (Fig 2.2b). Machining was carried, using CNC EDM, for 0.8 mm distance from top surface so that it would end at 0.1 mm above thermocouple. For the analysis purpose, average of maximum temperatures reached during experiments was taken into consideration.

## 2.5 Force Measurement

To measure the cutting force, octagonal type of dynamometer was used. Schematic diagram and circuit connections are as shown in the Fig. 2.6-2.7.

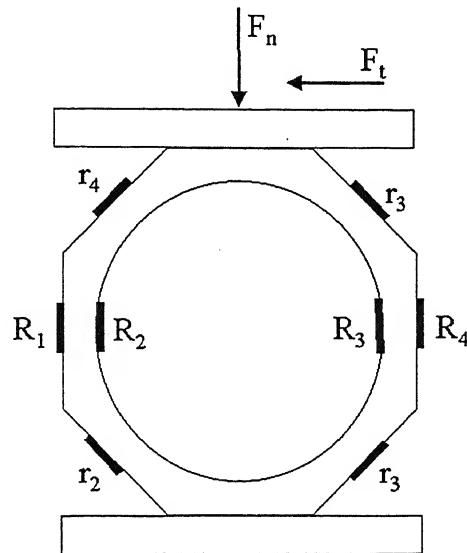


Fig 2.6 Octagonal ring type dynamometer for measurement of forces

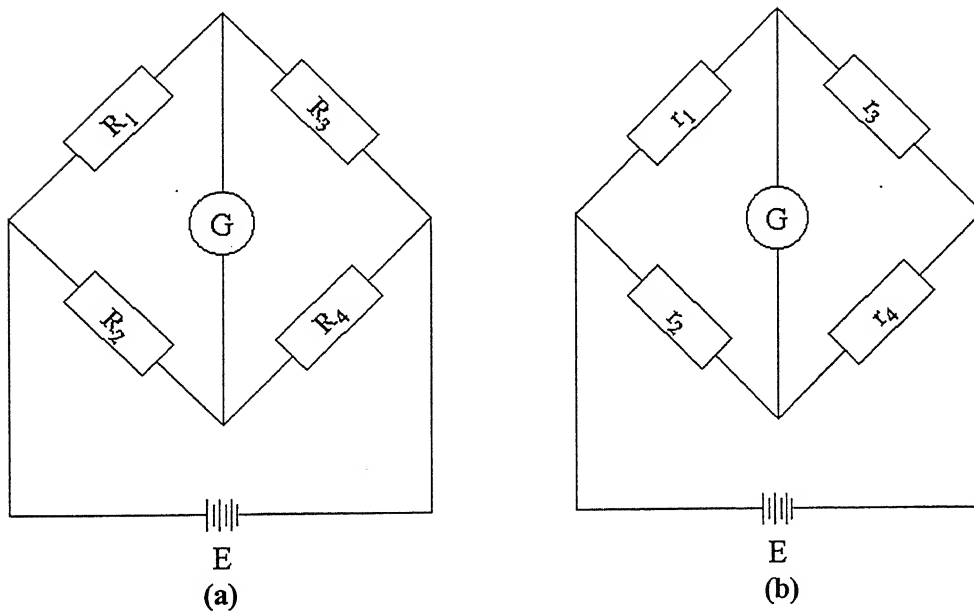
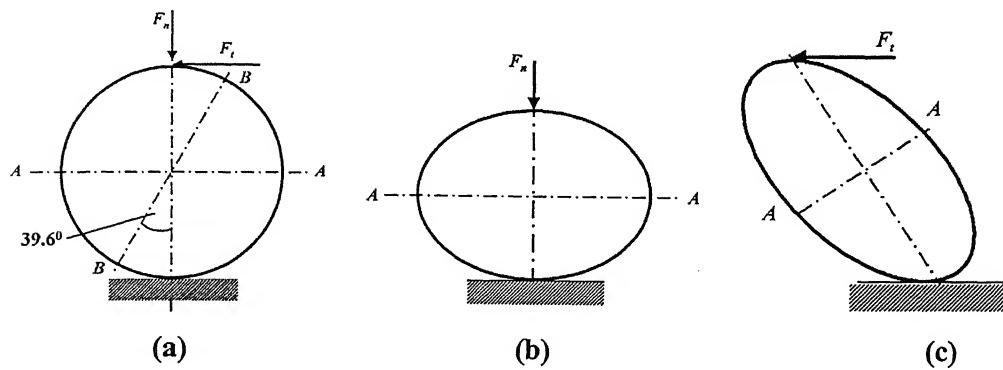


Fig 2.7 Circuit diagrams for measurement of (a)  $F_n$  and (b)  $F_t$

This dynamometer uses the strain gauge property of changing resistance when strained due to external forces. The strain gauges are mounted in such a manner that they form arms of the Wheatstone bridge. A change in resistance of gauges causes

loss of balance of bridge and output voltage signal is thus obtained. This output can be calibrated with applied force. Basically, to form a bridge, strain rings are ideal because they provide a high ratio of stiffness at the same time they possess adequate stability against buckling.



**Fig. 2.8 Circular strain ring showing the type of deformation produced.**

A thin metal ring of radius  $r$ , thickness  $t$ , and axial width  $b$  is shown in fig 2.8a. The ring is fixed at the bottom while a radial force  $F_n$  and a tangential force  $F_t$  are applied at the top. When only  $F_n$  is applied, the ring will deform as in Fig. 2.8b.

From thin ring elastic theory [35], the strain at the inside and outside surfaces of the rings at points A

$$e_A = \pm \frac{1.09 F_n r}{E b t^2}$$

while the strain at the point B ( $39.6^\circ$  from the vertical axis) is zero. When only  $F_t$  is applied (Fig. 2.8c) the strain at A is zero while the strain at B is

$$e_B = \pm \frac{1.09 F_t r}{E b t^2}$$

Thus, by placing strain gauges at the inside and outside surfaces of a ring at points A and B, it is possible to separate and measure  $F_t$  and  $F_n$  components of forces. Thus, if the inside and outside gauges at A are mounted in the opposite arms of a Wheatstone bridge then we can find  $F_t$  in terms of output voltage obtained. Similarly, the gauges at B are only sensitive to changes in  $F_t$ .

Octagonal rings are preferred over circular ones because of former's high stiffness. The dynamometer was calibrated using dead weights. The Calibration curves obtained are presented in the Appendix B.

## 2.6 Experimentation for EDM with rotating disc

EDDG is a hybrid process with EDM and conventional grinding as its constituents. Effort has been made to compare process performance of EDDG with EDM so that its feasibility could be tested. It was mandatory to perform the experiments with EDM under the same conditions with which EDDG experiments were performed. It was not possible to use metal bonded diamond wheel for experimentation of EDM action only since abrasion action was unavoidable. A special disc was manufactured having body of same material of that of diamond wheels. Only difference being that metal bond with diamond abrasive was replaced with bronze ring. For this purpose previously worn out wheel was used. This disc was then used on the same set-up used for EDDG experimentation.

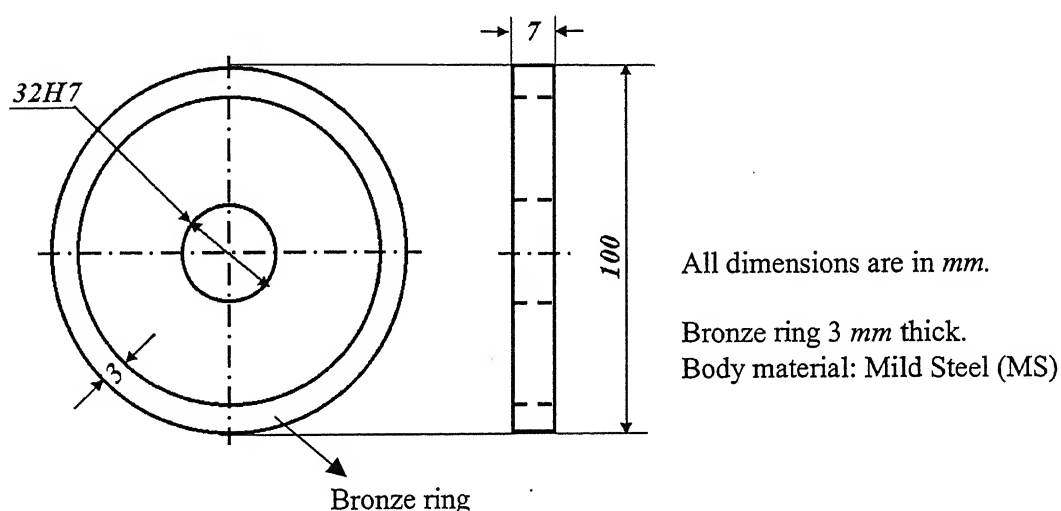


Fig. 2.9 A disc used for EDM experiments

Experiments were conducted under same process parameters that were used for EDDG experiments. Responses measured were temperature of the workpiece, material removal rate and, ultimately using all the measured data specific energy was calculated. Details will be discussed in later chapters.

# Chapter 3

## Parametric Analysis of Temperature and Material Removal Rate in EDDG

---

Experimentation is performed as per precautions and methodology discussed in chapter 2. Experiments are carried out using full factorial design for analyzing the responses, i.e., temperature, and material removal rate. The results are reported and corresponding analysis is presented in the following sections.

### 3.1 Experimental Results

As discussed in **Chapter 2**, full factorial design for 3 factors namely, current, wheel speed and pulse on-time, each at 3 levels, is presented below. Here, level of each factor is denoted by a coded variable. Calculations for coded variables is presented below:

$$\text{Current: } \text{code} = \frac{I - 13}{6} \text{ where } I = 7 \text{ to } 19A;$$

$$\text{Wheel Speed: } \text{code} = \frac{V_s - 5}{2.5} \text{ where } V_s = 2.5 \text{ to } 7.5\text{m/s}$$

$$\text{Pulse on-time: } \text{code} = \frac{T_{on} - 200}{100} \text{ where } T_{on} = 100 \text{ to } 300\mu\text{s}$$

27 experiments were conducted as per plan given in **Table 3.1**. Average of maximum temperatures reached are taken as response. A sample recorder output is as shown in **Fig. 3.1**. Output signal from thermocouple is in terms of millivolts. For analysis purpose, the sum of every peak (**Fig. 3.1**) in the output signal were made and then averaged. Using calibration curve (**Fig. A.1**), voltage output was converted into temperature.

$$\text{Avg. Temperature} = \frac{\text{Sum of peak temperatures during machining period}}{\text{Number of peaks}}$$

Material removal rate is calculated by measuring the weight of specimen before and after experiments and dividing the weight loss by corresponding

machining time. A digital balance was used for weight measurement having least count equal to 1 mg.

Taking into consideration non-linearity of the responses, second order polynomial was decided to fit into observations. To fit a second order model, it is mandatory to have each factor at minimum 3 levels. Experimental plan followed satisfies this condition. Second order polynomial to be fitted can be written as:

$$y = b_0 + \sum_{i=1}^n b_i x_i + \sum_{i=1}^n b_{ii} x_i^2 + \sum_{i < j} b_{ij} x_i x_j$$

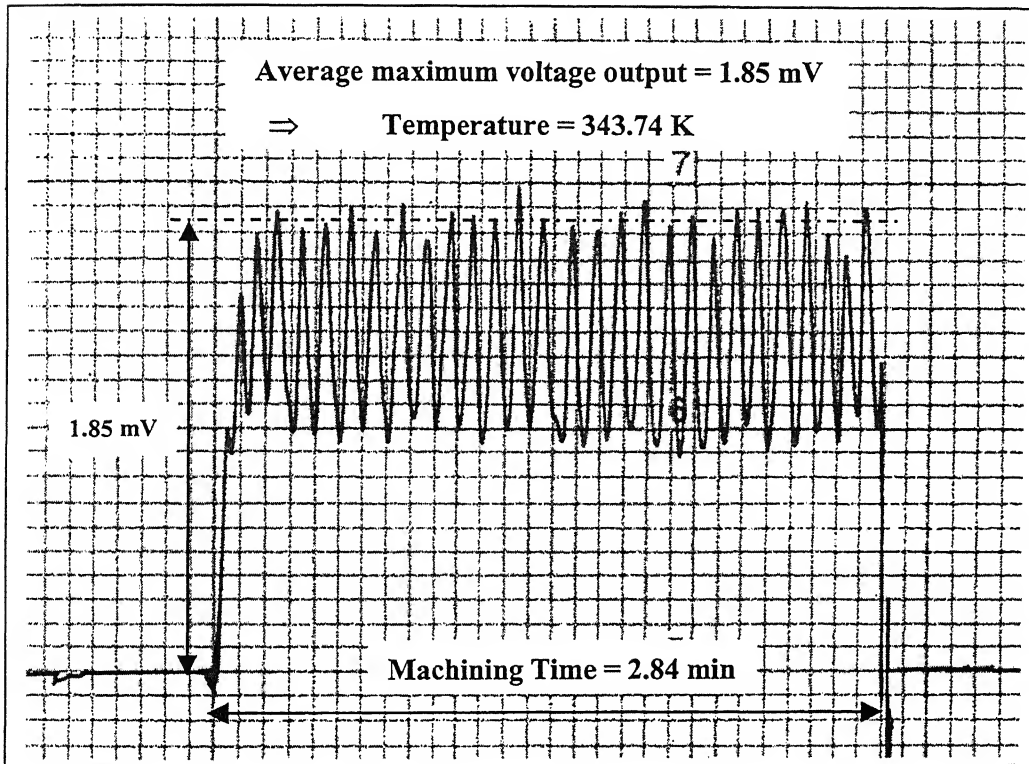


**Fig. 3.1 Sample Recorder Output (Scanned)**  
( $I = 13$  A,  $V_s = 2.5$  m/s,  $T_{on} = 100$   $\mu$ s)

By the regression theory presented in Section 2.3.1, a second order regression model was developed. Next step is ANOVA for regression equations. Results of ANOVA are presented in Table 3.2-3.3.

Calculations of regression coefficients and subsequent ANOVA were done using MINITAB software ([www.minitab.com](http://www.minitab.com)).

Exp. No.	I (A)	V <sub>s</sub> (m/s)	T <sub>on</sub> (μs)	T (K) (Exp.)	T' (K) (Eq.)	MRR (g/min) (Exp.)	MRR' (g/min) (Eq.)
1	-1	-1	-1	328.13	328.24	0.025	0.013
2	-1	-1	0	332.08	329.71	0.021	0.025
3	-1	-1	1	328.13	327.24	0.023	0.029
4	-1	0	-1	315.87	313.79	0.072	0.066
5	-1	0	0	314.47	316.86	0.052	0.070
6	-1	0	1	312.56	315.99	0.06	0.067
7	-1	1	-1	309.21	310.26	0.103	0.095
8	-1	1	0	314.74	314.93	0.079	0.092
9	-1	1	1	317.15	315.66	0.096	0.080
10	0	-1	-1	343.74	347.36	0.092	0.096
11	0	-1	0	355.48	351.91	0.142	0.138
12	0	-1	1	351.15	352.52	0.178	0.173
13	0	0	-1	329.32	332.85	0.144	0.149
14	0	0	0	341.14	339.00	0.186	0.183
15	0	0	1	339.18	341.21	0.216	0.210
16	0	1	-1	328.25	329.26	0.163	0.177
17	0	1	0	343.16	337.01	0.195	0.204
18	0	1	1	340.07	340.82	0.233	0.223
19	1	-1	-1	355.21	352.00	0.249	0.256
20	1	-1	0	349.22	359.63	0.311	0.328
21	1	-1	1	368.36	363.32	0.405	0.392
22	1	0	-1	343.72	337.43	0.309	0.308
23	1	0	0	346.88	346.66	0.400	0.372
24	1	0	1	352.14	351.95	0.410	0.429
25	1	1	-1	331.06	333.78	0.335	0.336
26	1	1	0	342.71	344.61	0.415	0.393
27	1	1	1	351.03	351.50	0.420	0.442

Table 3.1  $3^3$  full factorial design (Voltage = 40 V and duty factor = 0.64).

Regression equations fitted are as given below

- For Temperature:

$$T = 339 + 14.9I - 7.45V_s + 4.18T_{on} - 7.24I^2 + 5.46V_s^2 - 1.97T_{on}^2 - 0.06IV_s - 1.6V_sT_{on} + 3.08IT_{on} \dots\dots (3.1)$$

- For Material Removal Rate:

$$MRR = 0.183 + 0.151I + 0.0329V_s + 0.0305T_{on} + 0.0382I^2 - 0.0118V_s^2 - 0.00383T_{on}^2 - 0.00033IV_s - 0.00767V_sT_{on} + 0.0302IT_{on} \dots\dots (3.2)$$

Next step is to test the significance of the regression equations fitted for temperature and material removal rate. ANOVA technique is based on  $F$ -distribution test. ANOVA tables prepared are as presented in Table 3.2 and Table 3.3. For the analysis purpose, confidence level of 95 % is chosen. It means that  $\alpha$ -error associated will be 0.05. It is a probability of finding a significant association when one does not really exists. It is normal practice to use 0.05 as  $\alpha$ -error.

Source	DOF	SS	MS	$F_0$	$P$	$F_{(9,17,0.05)}$
Regression	9	5964.92	662.77	35.80	0.000	2.49
Residual error	17	314.76	18.52			
Total	26	6279.68				

**Table 3.2 ANOVA for temperature regression equation.**

In case of temperature regression equation,  $F$ -statistic has value 35.80. Now, critical value of  $F$ -distribution at 95% confidence level can be found from statistical tables. Critical value of  $F$  for temperature regression equation is found to be 2.49 which is less than  $F_0 (=35.80)$ . Also, in case of MRR regression equation,  $F_0$  has value 212.05, which is greater than critical value of  $F$  i.e. 2.49. Also,  $P$ -value based estimation is also presented in the table.  $P$ -value obtained from the ANOVA table should be less than  $\alpha$ -error chosen (i.e. 0.05). In both cases,  $P$  has value almost equal to zero, which is less than 0.05 i.e.  $\alpha$ -error.

Thus from the theory presented in Section 2.3.2, we can conclude that both the regression equations are significant in explaining the relationship between their respective responses (i.e. MRR and temperature) and input factors.

Source	DOF	SS	MS	$F_0$	$P$	$F_{(9,17,0.05)}$
Regression	9	0.469566	0.052174	212.05	0.000	2.49
Residual error	17	0.004183	0.002460			
Total	26	0.473749				

**Table 3.3 ANOVA for MRR regression equation.**

Using equations 3.1 and 3.2, responses are calculated and are given in Table 3.1. Using the calculated responses, figures 3.5-3.13 have been plotted. Based on observations tabulated in Table 3.1, main effects are presented in Fig. 3.2 and Fig



3.3. These graphs are prepared by taking averages of responses at each level of a particular factor. These graphs give information how the input parameters (current, wheel speed and pulse on-time) affect the process response (temperature and material removal rate) on the same scale. It is quite obvious that it will not give any information about interactions among the factors. For that purpose, detailed graphical presentation is given in the Section 3.2.

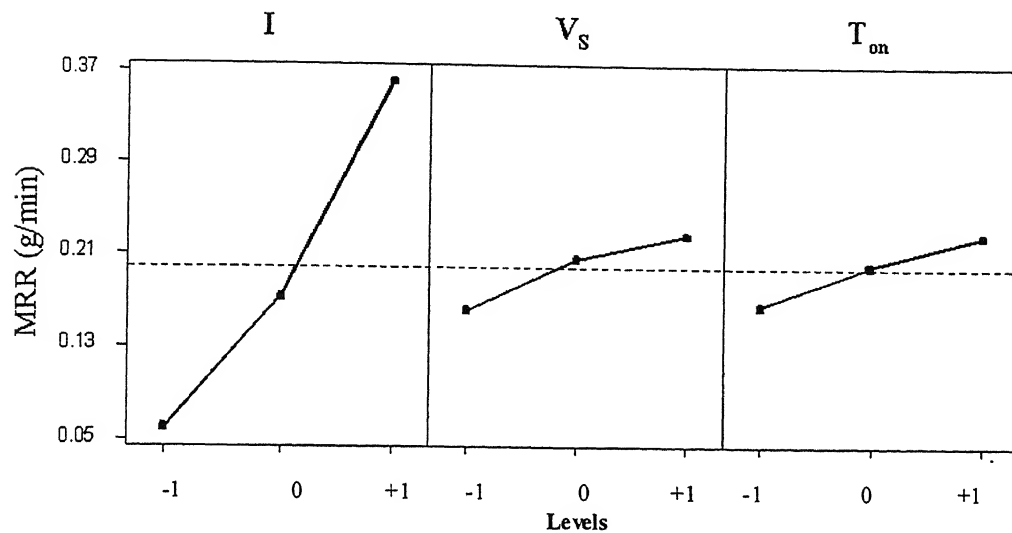


Fig. 3.2 Main effects for MRR

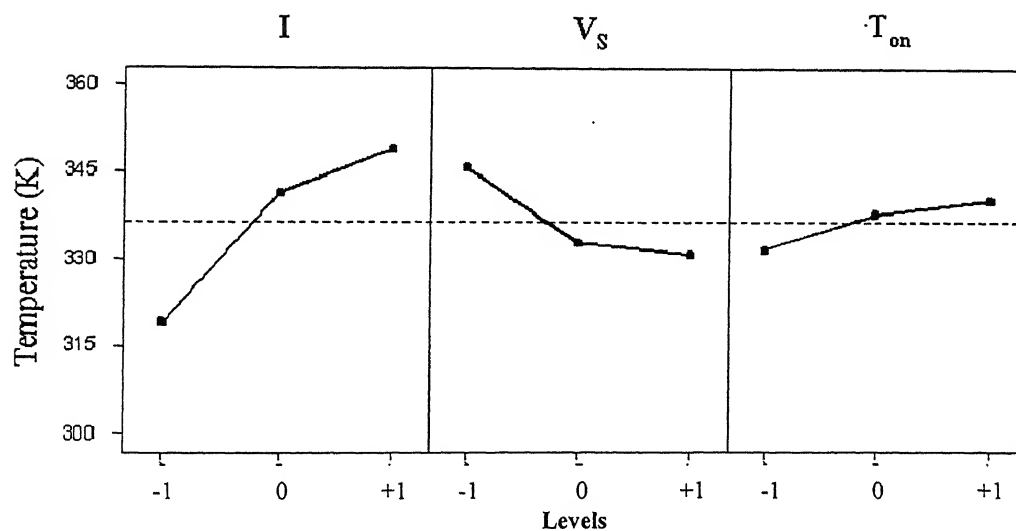


Fig. 3.3 Main effects for Temperature

### 3.2 Discussion

Before analyzing the results tabulated above, it would be worthwhile to present mechanism of EDM action. Complexity of EDM action, particularly a discharge phenomenon has thrown challenge before researchers to understand the basics behind it.

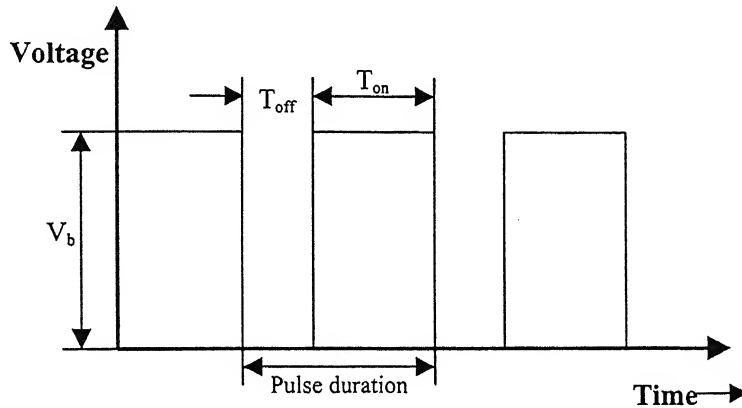


Fig. 3.4 Pulsed D.C. Voltage

In EDM, there are two electrodes, a cathode, and an anode, separated by a liquid dielectric. During operation, an applied voltage across a gap between electrodes causes dielectric to breakdown. A plasma channel, surrounded by vapor bubble, develops and expands during “on-time” of pulse, which is usually of the order of  $100 \mu\text{s}$  (Fig. 3.4). Unlike a gas, the surrounding, dense liquid dielectric restricts the plasma growth, concentrating the input energy  $VIt\tau$  in a very small volume. During this on-time the high-energy plasma melts both electrodes by thermal conduction, but limited electrode vaporization occurs due to high plasma pressures. Furthermore, the anode first melts rapidly due to absorption of fast moving electrons at the start of the pulse, but then begins to resolidify after a few microseconds. Melting of the cathode is delayed in time by one or two orders of magnitude beyond that of anode due to the lower mobility of the positive ions [36]. Moreover, the plasma radius at the cathode is also much smaller, caused due to emitting electrons (Fig. 3.5). At the end of the on-time, a off-time (i.e. power is terminated to the machine) period begins. During this period, a violent collapse of the plasma channel and the vapor bubbles occur, causing a superheated, molten liquid on the surface of both the electrodes to explode into the liquid dielectric. While some of the material is carried away by the dielectric, the remainder of the melt in the cavities resolidifies in place, called as *recast layer*.

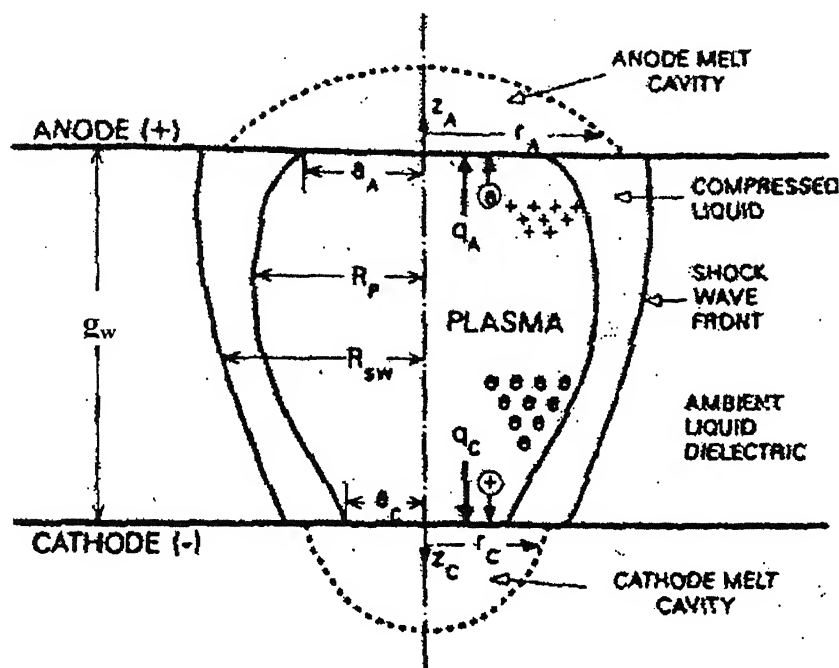
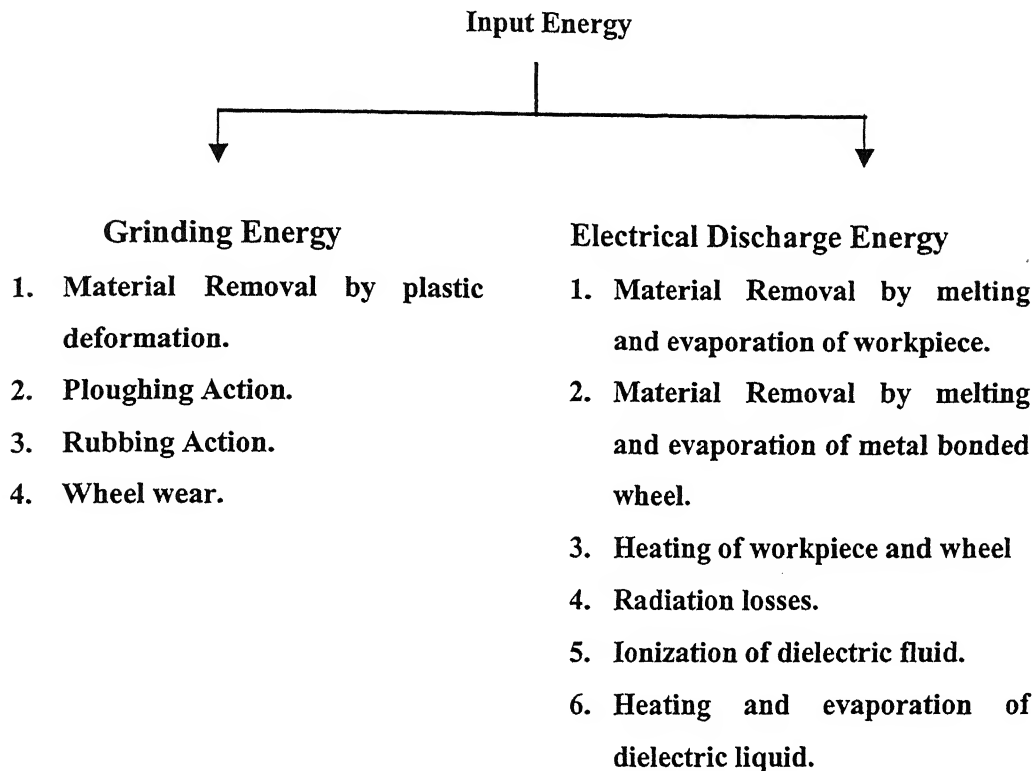


Fig. 3.5 Plasma channel profile during EDM.

During discharge phase, it has been commonly accepted that debris formed play important role in the development of discharge. The debris in the machining gap consists of products of dielectric decomposition and eroded metallic particles.

1. The presence of debris particles in the gap increases the local electrical-field strength and local current densities leading to the reduction of ignition delay (The ignition delay time is the time, which passes between the application of the voltage between the electrode and workpiece, and the ignition or sparking. [37]). The nature and the extent of ignition delay dictate the changes in the types of discharge and the energy of each discharge which is related to erosion rate [38].
2. With increased pulse energy, the size of the debris particle increases. The incidence of discharges on the debris particles would break them down into smaller size particles. This phenomenon is termed as "secondary discharge". It appears in the absence of effective flushing.[7]
3. Although, debris particles are useful in activation of discharges, too much concentration leads to "arcing" phenomena in place of sparking. Such arcing only heats the material in place of removing it by erosion.

Following chart gives energy utilization in EDDG



With this mechanism of material removal in EDM, effects of process parameters of EDDG are analyzed in following sections.

### 3.2.1 Effect of pulse current

From Fig. 3.6-Fig. 3.8, it is clear that as current increases, MRR and temperature increase. As current increases EDM action dominates over grinding. Grinding assists EDM in removing debris. It also decreases the chances of resolidification of molten material.

Critical rake angle of abrasive grains is an important consideration while analyzing improved MRR in EDDG. The critical rake angle for a particular material is primarily dependent on the coefficient of friction between contacting surfaces. It has been observed that an increase in temperature of the workpiece causes shift in the critical rake angle towards the more negative values in slow-speed abrasion of steel [27]. In EDDG, introduction of the electrical sparks in the grinding zone causes increase in temperature of workpiece. Rather, we can say that region

which would be machined by abrasive grain (diamond in present case) gets heated before actually machined. Thus, ultimately abrasive grains pose highly negative rake angles to the workpiece. Temperature is found to be increased due to the fact that increases in current leads to increase in input energy ( $VI\tau$ ). This input energy is utilized in many ways like melting and evaporation of work and electrode, and losses in radiation. From the main effects plot (Fig. 3.2-3.3), it is evident that current is most dominant factor in increasing MRR and temperature.

From graphs (Fig. 3.6-3.8), at lower values of current, increase in MRR and temperature with increase in pulse on-time is not much significant as compared with increase in MRR and temperature with increase in on-time at higher values of current. It can be said that the effect of on-time is not much significant when compared with its effect at higher current because, at higher currents EDDG is in EDM dominant mode. It can also be termed as “synergetic interaction”. (Fig 2.4)

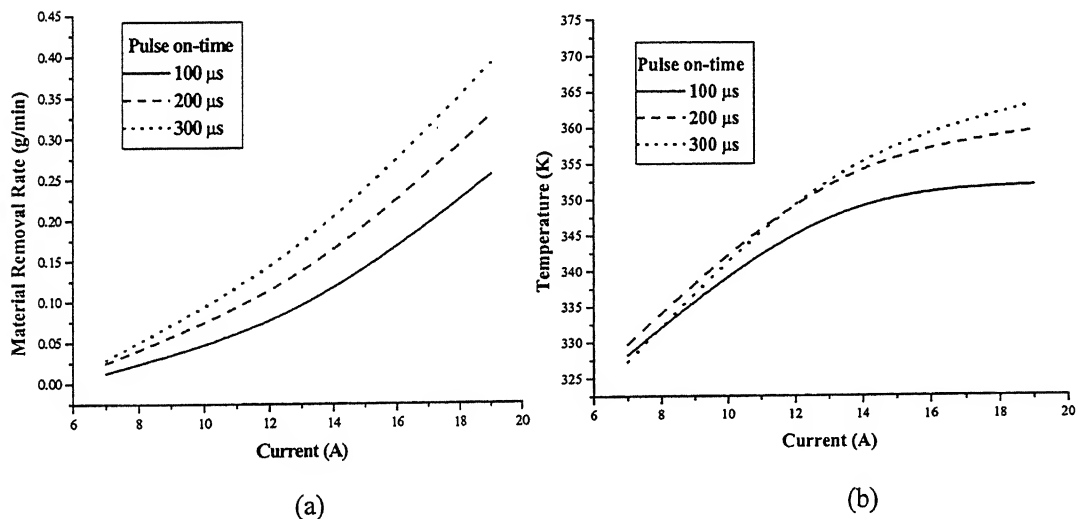


Fig 3.6 Effect of pulse current on (a) Material Removal Rate and (b) Temperature at wheel speed = 2.5 m/s.

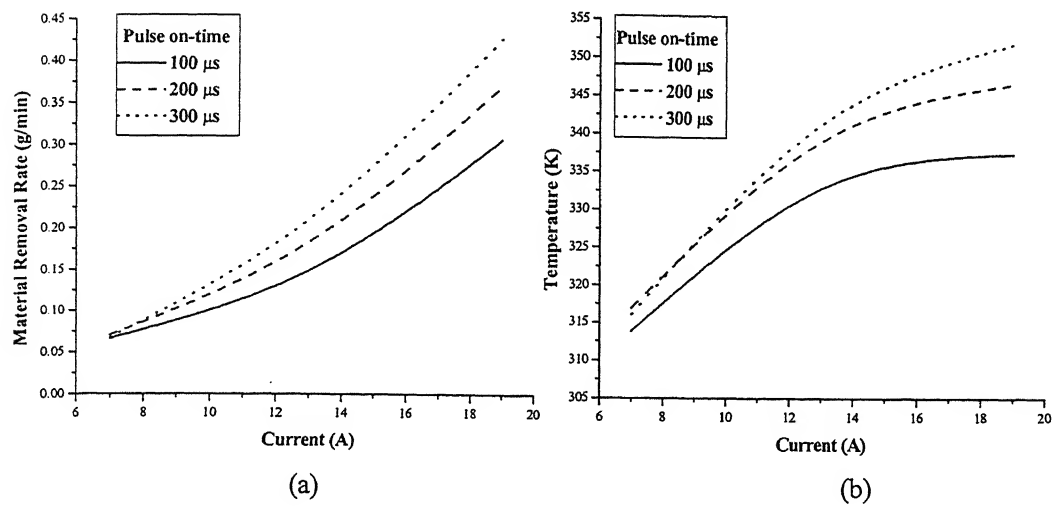


Fig 3.7 Effect of pulse current on (a) Material Removal Rate and (b) Temperature at wheel speed = 5 m/s

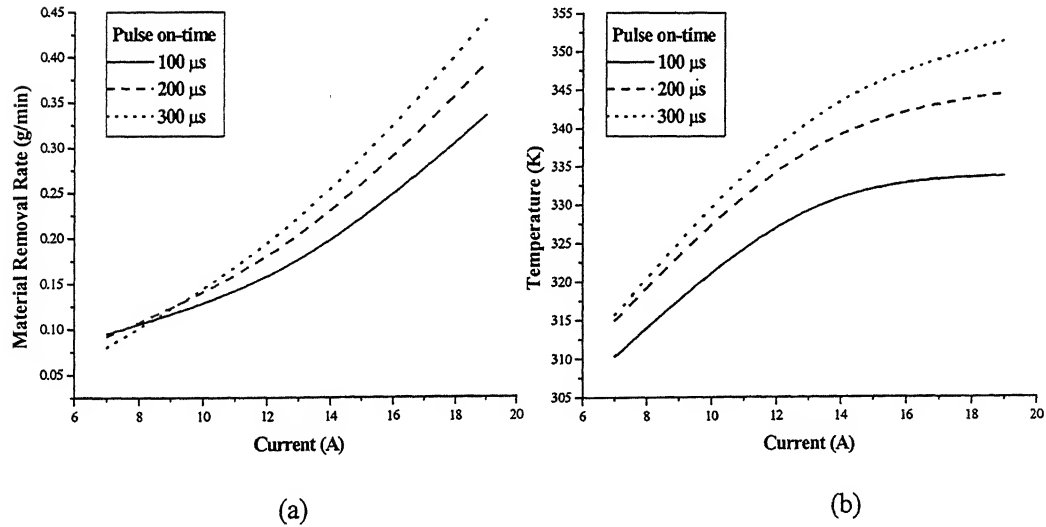


Fig 3.8 Effect of pulse current on (a) Material Removal Rate and (b) Temperature at wheel speed = 7.5 m/s

### 3.2.2 Effect of wheel speed

Wheel speed (cutting speed) is a grinding parameter influencing the responses. MRR increases as wheel speed increases but temperature decreases. (Fig. 3.10- 3.13)

Improvement in MRR can be attributed to the increased abrasive action due to increase in cutting speed. Also, for a given current and pulse on-time (i.e. for given discharge energy), molten material is being rapidly thrown away from the working gap. This ejection due to grinding might be faster than the speed of heat front travelling into the workpiece. Also, increased speed results in improved flushing of dielectric. This action leads to rapid cooling of work leading to lowering the temperature of workpiece (Fig. 3.3)

MRR depends upon the degree of interaction between the wheel and the work. Hence, dynamics of the gap-width is important from MRR point of view. With increasing wheel speed, the reduced contamination at the gap results in decreasing gap-width which would increase the undeformed chip-thickness (Fig. 3.9). This has the effect of increasing the MRR with respect to wheel speed.

Arcing in EDM occurs when the plasma channel takes the same path as that of the previous pulse, which is not completely deionised. Subsequently, new gaseous path required for a spark discharge is not formed and the spark spot distribution all over the machining area is hampered. Such localization of the discharge is nothing but “an arc”. Effective material removal is due to spark only. Arcs imply process instability. Inadequate flushing leads growth of the conducting particles to such a concentration that short circuits and arcs dominate sparks. An ultimate result is low MRR. In EDDG, rotating wheel minimizes such condition. Hence, MRR gets increased.

It has been observed that, at a particular current, rate of increase in MRR falls as wheel speed increases. Affinity of diamonds with steel has been discussed in Ref. 31. Diamond grains wear rapidly owing to graphitization of diamond, with iron as catalyst. The rate of reaction depends upon temperature at the grain work interface. Rate of fall of temperature with increasing wheel speed (Fig. 3.10b) is found to be decreased. It further causes wear of grains. The implication of wear-flat formation is decrease in uncut chip thickness (Fig. 3.9). Hence, with the formation of wear flats, a number of grains which hitherto have been actively involved in material removal, tend to just plough and displace but not remove material. This causes fall in rate of increase in MRR with wheel speed.

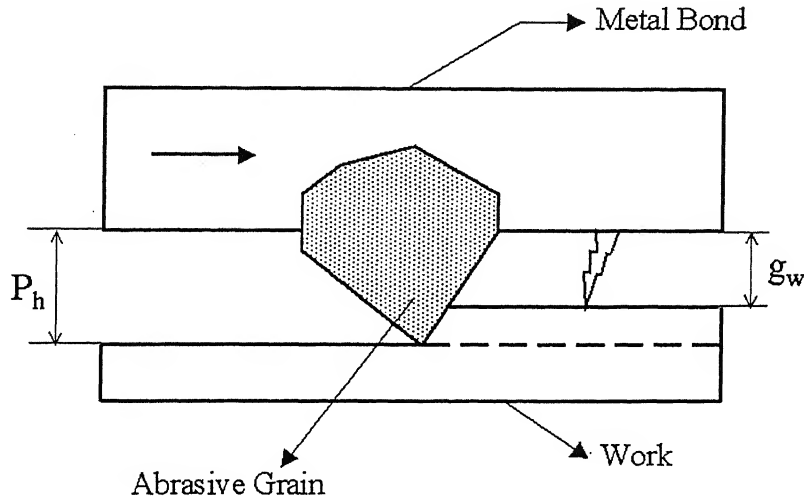


**Fig. 3.9 Schematic representation of the wheel-work interface in EDDG**

So, higher speed may reduce temperature and improve MRR. But, for particular pulse energy there is a limit to increase MRR by increasing the wheel speed. This phenomenon is due to arc instability caused by forced flushing through the gap. Although, in the present study no such instability was observed. It simply implies that chosen range of wheel speed (2.5 m/s- 7.5 m/s) is suitable for operating EDDG.

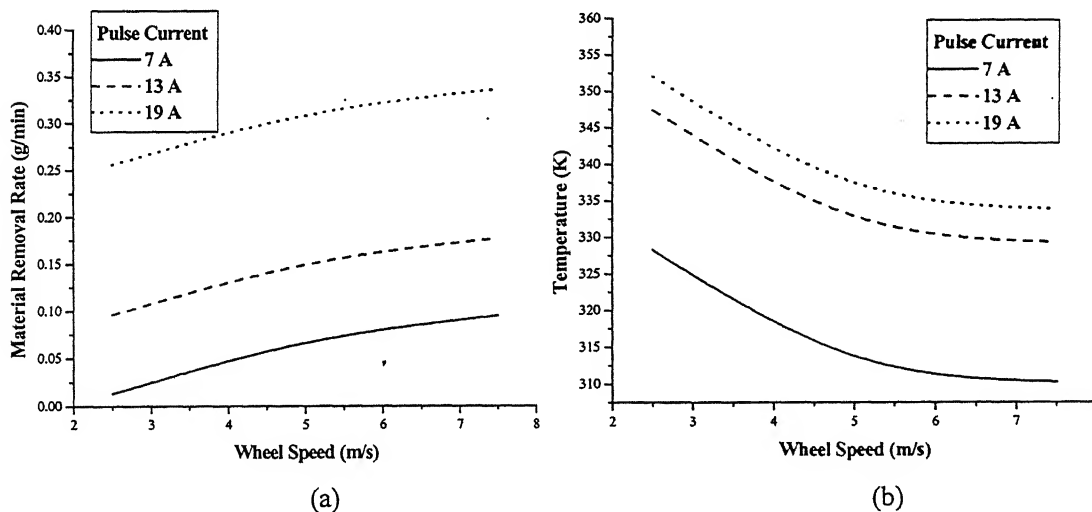


**Fig 3.10 Effect of wheel speed on (a) Material Removal Rate and (b) Temperature at pulse on-time = 100  $\mu$ s.**



### 3.2.3 Effect of pulse on-time

MRR and temperature of the workpiece increase with increase in pulse on-time (Fig. 3.13-3.15). Although, experimental points shows quite complex trends (Table 3.1). This is due to the fact that enough time is available for conduction of heat into the interior of work, which would result in softening of a larger volume of workpiece. This softening of the workpiece reduces the attritious wear of grits resulting in higher protrusion height, and hence higher depth of penetration. Since MRR is related to the depth of penetration, it increases with increase in pulse on-time. But it should be noted that this increase in MRR is not much significant as compared to MRR rise due to increase in current. Varying on-time does not really increase input discharge energy (since input discharge energy depends on voltage, current, duty factor and machining time).

It has been observed that mechanism of material removal in EDM is thermal erosion when pulses are of shorter duration and when pulses are of longer duration material removal takes place by melting and evaporation [39]. Also, dependence of MRR on on-time is governed by multiple phenomena taking place during discharges. It has been reported that, for longer pulses, MRR value may get reduced [39]. Such behavior can be explained by following points

- The discharge channel has a finite width causing a heat source distributed on a finite area rather than a point source;
- Ionization and excitation of the evaporated metal and the dielectric fluid take place requiring energy, thus decreasing the energy available for melting.
- A certain part of the eroded material fuses back in the creator after completion of the pulse.

Thus, complex nature of the above phenomena leads to quite unpredictable nature of responses, which is evident from graphs shown. Such behavior has also been reported in Ref. 18 and Ref. 26.

It can be seen from Fig. 3.13-3.15 that the wheel speed and the pulse on-time show “*anti-synergetic interaction*” (Fig.2.4).

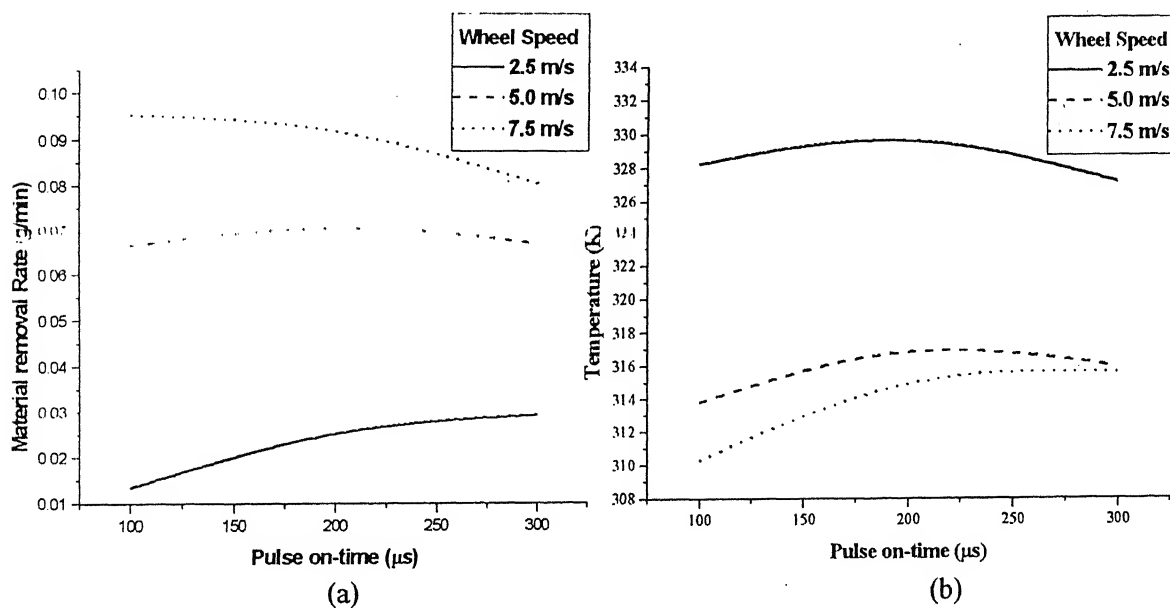


**Fig 3.13 Effect of pulse on-time on (a) Material Removal Rate and (b) Temperature at pulse current = 7 A.**

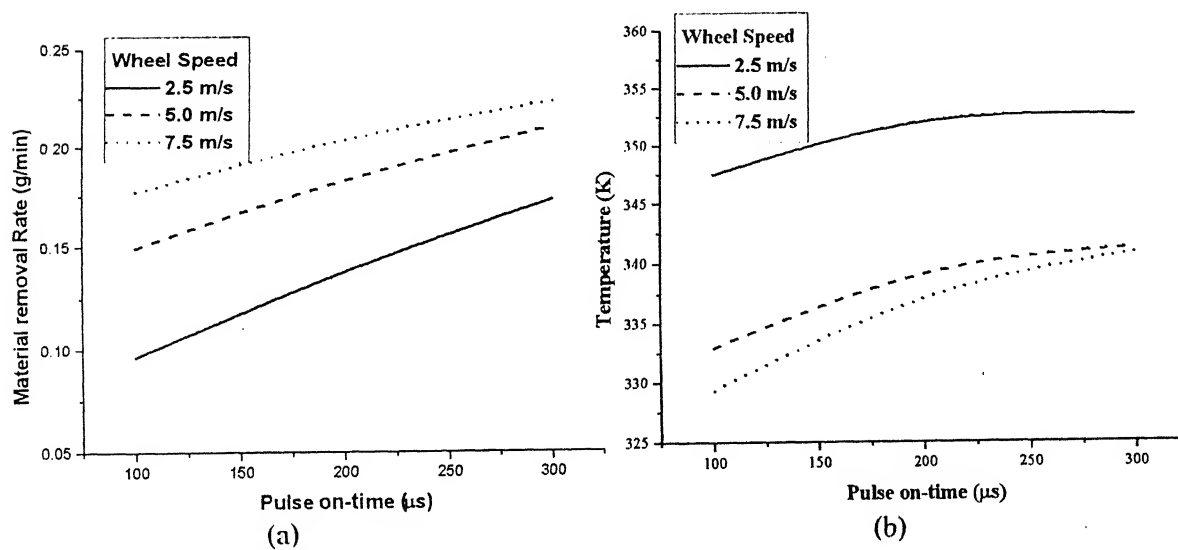


**Fig 3.14 Effect of pulse on-time on (a) Material Removal Rate and (b) Temperature at pulse current = 13 A**

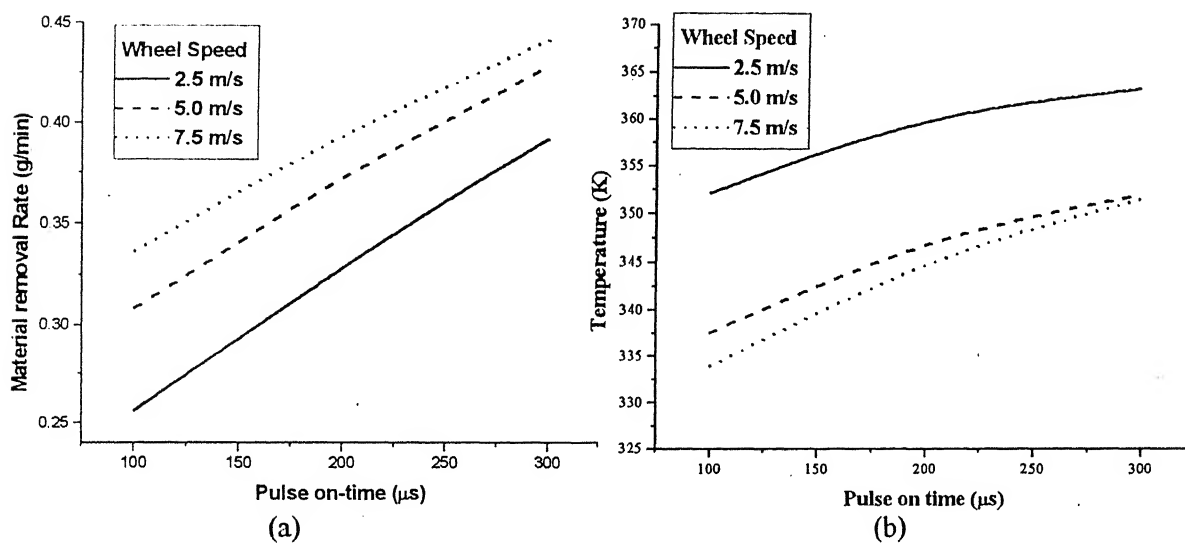


**Fig 3.15 Effect of pulse on-time on (a) Material Removal Rate and (b) Temperature at pulse current = 19 A**

# Chapter 4

## Specific Energy in EDDG

---

Feasibility of any process can be judged using various parameters like MRR, tool wear, dimensional accuracy, etc. Electrodischarge machining (EDM) is known for its inefficiency. It would be interesting to see how the combination of EDM and grinding in EDDG plays role in the context of specific energy. This chapter throws some light on specific energy in EDDG. Also, comparison is also presented with EDM using rotating disc electrode.

### 4.1 Specific Energy Calculation

Specific energy of any material removal process can be defined as *amount of energy required to remove unit volume (or unit mass) of material being machined*.

$$\text{Specific Energy} = \frac{\text{Amount of energy supplied in a specified period of time}}{\text{Amount of material removed in same period of time}}$$

EDDG being hybrid process comprising of EDM and grinding, we have to take into consideration energy supplied to both constituent processes.

$$\text{Grinding Power, } P_G = F_t V_s \dots \dots \dots (4.1)$$

where,  $F_t$  = Tangential force

$V_s$  = Cutting Speed

$$\text{Discharge Power, } P_D = VI \dots \dots \dots (4.2)$$

Let, machining is continued for a period of  $t$  and let  $\tau$  be duty cycle.

Hence, pulse will be ON for time =  $t\tau$

$\Rightarrow$  Energy supplied, during EDM, in time ' $t$ ', =  $(VI)(t\tau)$

Also, Grinding energy supplied in same time, =  $(F_t V_s)t$

$\Rightarrow$  Total Energy supplied during EDDG in time ' $t$ ',

$E = \text{Discharge Energy} + \text{Grinding Energy}$

$$E = (VI)(t\tau) + (F_t V_s)t$$

Let, amount of material removed during time 't' be 'W'

$$\begin{aligned} \therefore \text{Specific Energy in EDDG} &= \frac{E}{W} \\ &= \frac{(VI)(t\tau) + (F_t V_s)t}{W} \\ &= \frac{(VI)\tau + F_t V_s}{W/t} \end{aligned}$$

$$\boxed{\therefore \text{Specific Energy in EDDG} = \frac{(VI)\tau + F_t V_s}{MRR}} \dots\dots\dots (4.3)$$

While calculating specific energy in EDM with rotating disc, energy spent in rotating the disc is not taken into account. This is because, there is no physical contact between wheel and the workpiece in EDM with rotating disc. No material is removed due to rotation of the wheel as in the grinding. It has been found that, during EDDG, although mechanical abrasion takes place, grinding energy is very small as compared to discharge energy (Table B.1-B.4). Hence, in case of EDM with rotating disc it would be much smaller and neglected.

## 4.2 Experimental Results and Discussion

Following sections provide results of experiments conducted for calculating specific energy in EDDG. Attempt is also made to compare it with that of EDM with rotating disc electrode.

### 4.2.1 Specific EDDG Energy

Specific energy is an important concept in the field of machining science. Results of experimentation are presented in **Appendix B**. Analysis of results is presented in the following sections. Analysis has been done in the context of specific energy, as well as cutting force variation with corresponding temperature of the workpiece.

Basically, the material removal process in grinding is no different from that occurring in other metal cutting processes [40]. Individual abrasive grains that are in contact with the work due to frictional resistance experience cutting force in grinding. This resistance to motion of grain can be attributed to:

- The force required to shear the junction formed between work and grain, and
- The force needed to displace the material ahead of the grain.

These forces are influenced by the bulk physical properties of work material. The temperature of the workpiece plays a key role in defining the shear strength of the junction. It is because of the formation of adhesion junctions between the work and the grain at the point of contact, such phenomenon occurs due to cold-welding process [41].

In case of EDDG, following factors should be considered for analyzing the cutting force behavior.

1. Assistance of electrical discharges to the material removal process. A part of the material is removed by the electrical discharge before the abrasive grains cut the material.
2. The self-sharpening process of the grinding wheel is activated by the electrical discharges. In the absence of electrical discharges, it was observed that the metal bond of the grinding wheel hides most of the diamond grains. When discharges are applied, the diamond grains are not hidden by the bond metal [25].
3. Introduction of discharge in the working zone causes thermal softening of the work material.

### 4.2.1.1 Effect of pulse current

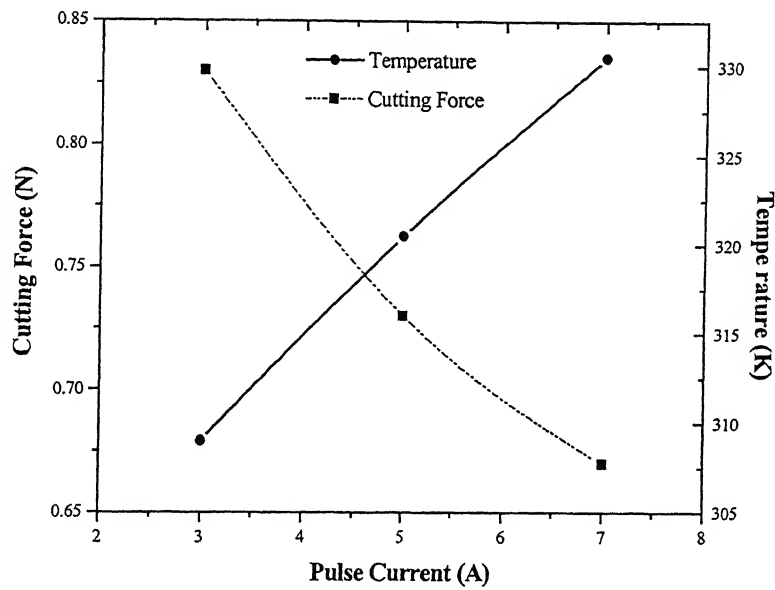


**Fig. 4.1** Effect of pulse current on cutting force and temperature  
(Wheel speed = 2.5 m/s; pulse on-time = 100  $\mu$ s; duty factor = 0.64; voltage = 40 V)

Increase in pulse current leads to decrease in cutting force (Fig. 4.1). This is clear from the above-discussed factors (Section 4.2.1). Increase in current implies increase in input heat energy and subsequent fall out is thermal softening of the work material. So, forces required to remove material will be lesser as current increases.

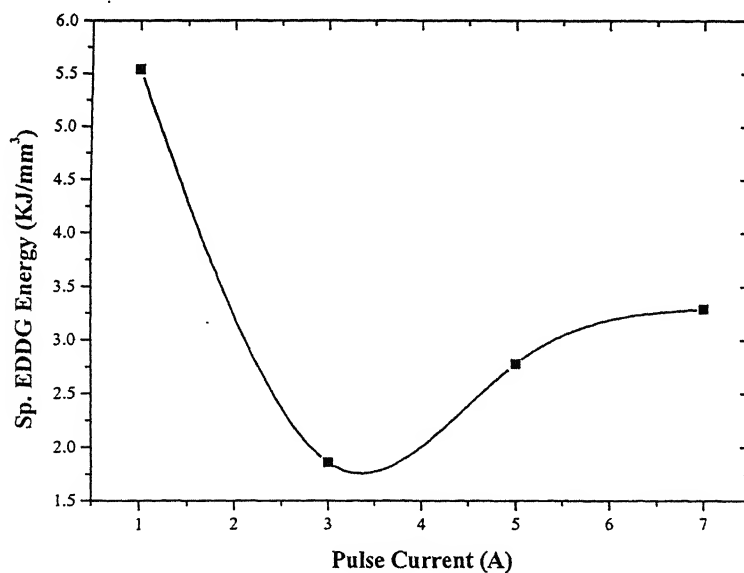


**Fig. 4.2** Effect of pulse current on specific EDDG energy  
(Wheel speed = 2.5 m/s; pulse on-time = 100  $\mu$ s; duty factor = 0.64; voltage = 40 V)

Specific EDDG energy versus current plot (Fig. 4.2) shows that as current increases, specific EDDG energy also increases, for currents 3A onwards. Highest specific energy at 1 A is mainly due to the lowest MRR at such low current (Table B.1). Material removal is predominantly by grinding. Up to 3A current, specific EDDG energy decreases due to increase in MRR with increase in current. Although, reduction in cutting force causes lesser amount of grinding energy, it is evident from the Tables B.1-B.4 that the discharge energy is dominating factor in defining specific EDDG energy. Increase in current leads to increased discharge energy input. But, very less part of discharge energy is actually utilized in material removal. Most of its part gets wasted in other phenomena like radiation loss, heating of workpiece and wheel, dielectric ionization and vaporization, etc. So, as current increases such losses also increase. Ultimately, it increases specific EDDG energy.

#### 4.2.1.2 Effect of wheel speed

It has been analyzed in Section 3.2.2 that the increase in wheel speed causes decrease in temperature. This reduction in temperature is the cause of lesser thermal softening of work material. It means that the increase in wheel speed should increase cutting force (Fig. 4.3). Also, cutting force in grinding varies directly with wheel speed. Such trend is evident from the plot shown in Fig. 4.3.

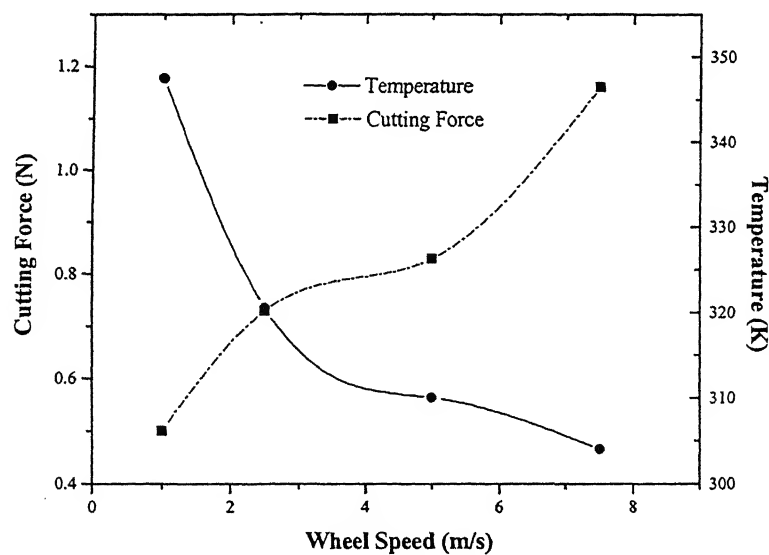
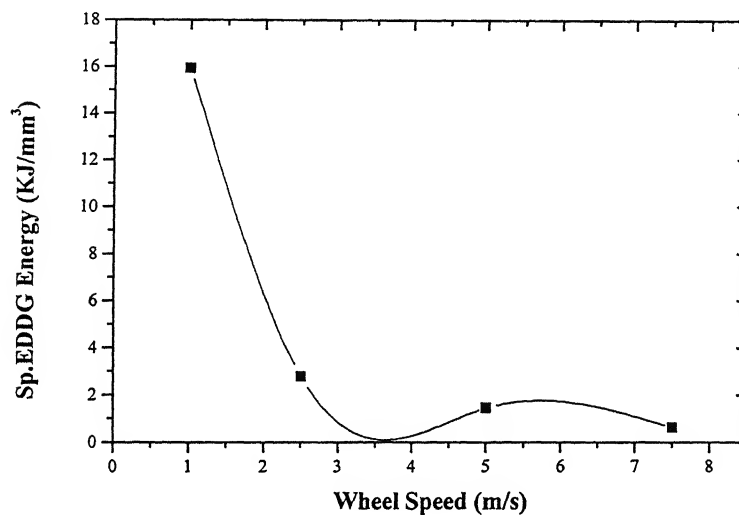


Fig. 4.3 Effect of wheel speed on cutting force and temperature  
(Pulse current = 7 A; pulse on-time = 100  $\mu$ s; duty factor = 0.64; voltage = 40 V)



Grinding energy increases with wheel speed, (Eq. 4.1). But, as discussed earlier, increase in grinding energy is not much significant as compared to discharge energy. It should be noted here that MRR significantly increases (Table B.2) with increase in wheel speed. Since MRR is important factor in characterizing specific EDDG energy, specific EDDG lowers with increase in wheel speed.



**Fig. 4.4 Effect of wheel speed on specific EDDG energy**  
(Pulse current = 7 A; pulse on-time = 100  $\mu$ s; duty factor = 0.64; voltage = 40 V)

#### 4.2.1.3 Effect of pulse on-time

Increase in pulse on-time indicates that the discharge will be on for more time span. It would give more time to heat source (i.e. discharge) to be in the working zone. From above graph (Fig. 4.5), it is clear that on-time increase leads to increase in temperature and obviously decrease in cutting force. Also, pulse on-time has a effective role in resharping of diamond grains. But, abnormal behavior is observed at pulse on-time equal to 200  $\mu$ s. (Fig. 3.10-3.12, and Fig. 4.5). Such trend can be attributed to the complex phenomena associated with pulse on-time, as discussed in detail in Section 3.2.3.

Increase in pulse on-time, actually has no influence on increase in discharge energy (Eq. 4.3). But, it improves MRR. Although, as discussed in Section 3.2.3,

effect of pulse on-time on MRR is of complex nature. The change in specific energy with a change in pulse on-time is presented in Fig. 4.6.

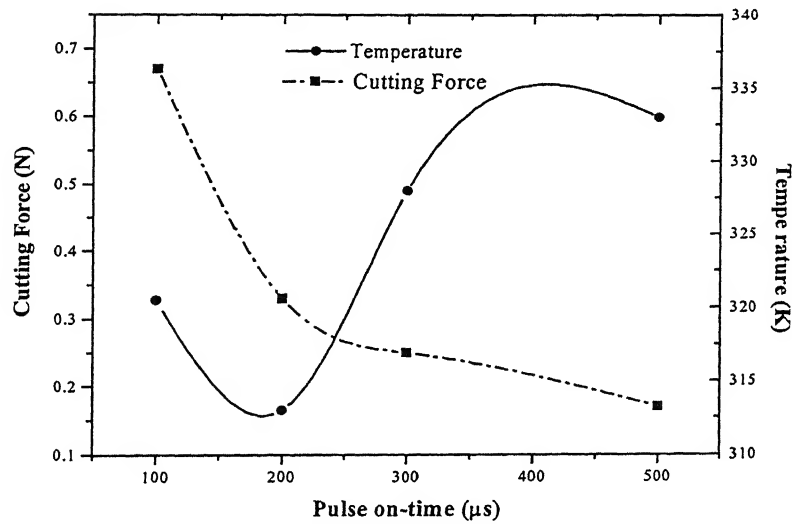


**Fig. 4.5 Effect of pulse on-time on cutting force and temperature**  
(Pulse current = 7 A: wheel speed = 2.5 m/s: duty factor = 0.64: voltage = 40 V)

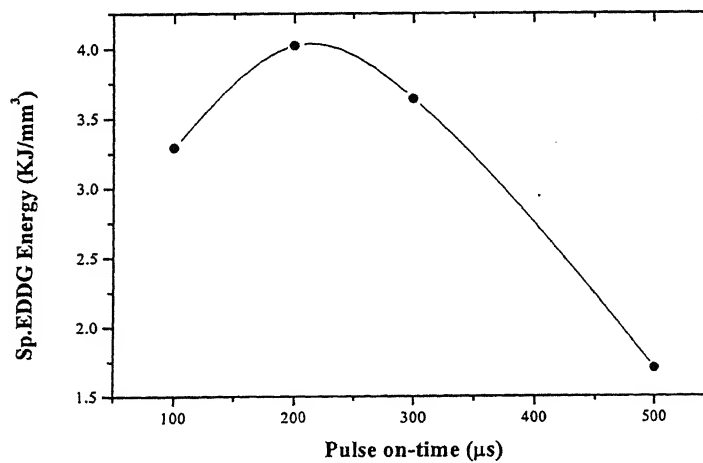


**Fig. 4.6 Effect of pulse on-time on sp. EDDG energy**  
(Pulse current = 7 A: wheel speed = 2.5 m/s: duty factor = 0.64: voltage = 40 V)

#### 4.2.1.4 Effect of duty factor

Duty factor defines the proportion of the on-time and the off-time for total pulse time. Increase in duty factor, for a fixed on-time, means lowering the off-time. Off-time is vital in the material removal mechanism since material gets melted during

on-time of the pulse and gets ejected out during off-time (section 3.2). Smaller duty factor, at a particular on-time, means longer off-time. It effects in less amount of energy supplied for entire machining time. From this, increase in duty factor (i.e. increase in discharge energy) should lead to increase in temperature. Above graph (Fig. 4.7) confirms this fact. But, it will be interesting here to note that cutting force increases as duty factor increases. It means that the thermal softening due to discharge action is not only cause of decrease in cutting force, but also there are other factors influencing cutting force. As mentioned earlier, increase in duty factor means shorter off periods. This must hamper proper ejection of molten material, forming resolidified layer. This layer is known for its high hardness. When diamond grain removes harder layer, it is obvious that more force is required. Hence, the trend of cutting force can be explained. But, this explanation also suggests that MRR should decrease with increase in duty factor due to resolidification (it is not always possible for each grain to remove this layer, wherever it does so, it does with high forces). From Table B.4, one can see a decrease in MRR with increase in duty factor. Thus, explanation is justified.

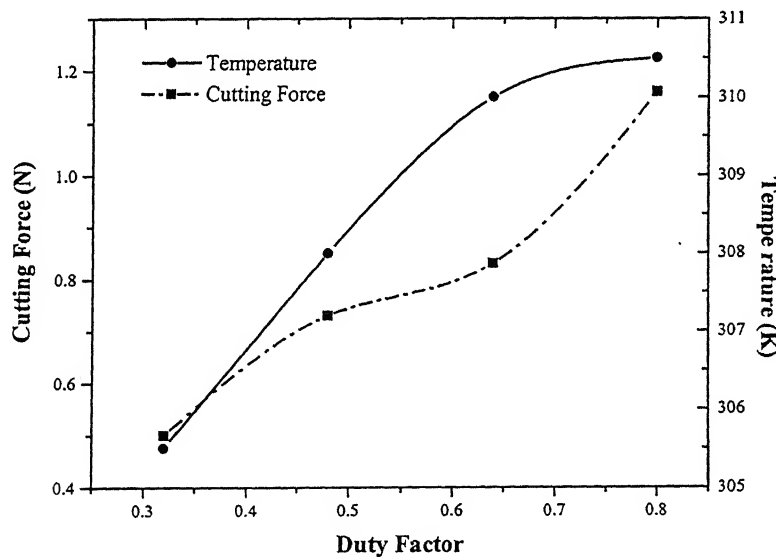
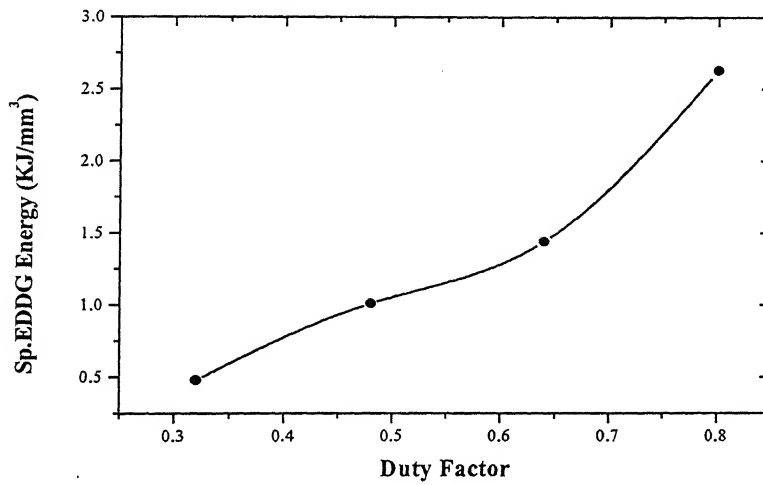


Fig. 4.7 Effect of duty factor on cutting force and temperature  
(Current = 5 A; wheel speed = 5 m/s; pulse on-time = 100  $\mu$ s; voltage = 40 V)

As far as specific EDDG energy is concerned, it is evident that increase in duty factor means increase in discharge energy. But, as discussed above, MRR decreases with increase in duty factor. Cutting forces are found to increase with

increase in duty factor. So, total energy input increases but MRR decreases. So, specific EDDG energy is found to be increased with increase in duty factor. This is depicted in the following graph (Fig. 4.8).



**Fig. 4.8 Effect of duty factor on specific EDDG energy**  
(Current = 5 A: wheel speed = 5 m/s: pulse on-time = 100  $\mu$ s: voltage = 40 V)

#### 4.2.2 Specific energy in EDM with rotating disc

As discussed in section 4.1, energy spent in rotating the disc is neglected, specific energy in EDM with rotating disc can be obtained from equation 4.3.

$$\therefore \text{Specific Energy in EDDG} = \frac{(VT)\tau}{MRR} \dots\dots\dots (4.4)$$

##### 4.2.2.1 Comparison of EDDG with EDM with rotating disc

EDM with rotating disc is a process near to EDDG. So, comparison between these two processes in the context of specific energy will be valuable while discussing feasibility of the EDDG.

Specific energy plot clearly shows wide gap between specific energy in EDDG and that of EDM with rotating disc. Also, specific energy in EDDG is found to be less. This suggests that EDDG is more efficient than EDM process in the context of specific energy. But, as pulse current increases, the specific energy values of two processes approach nearer to each other (Fig. 4.9). Effect of assistance of grinding goes on reducing as current increases. This is due to the fact that current increase

leads hybrid EDDG process towards EDM dominant mode. Effect of pulse on-time is also shown in graph below, (Fig. 4.10).

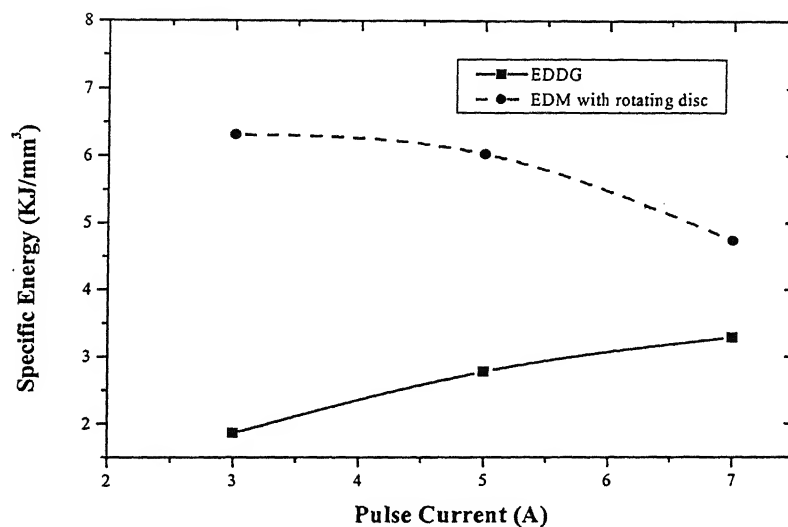


**Fig. 4.9 Specific energy in EDDG and EDM with rotating disc**  
(Disc speed = 2.5 m/s; pulse on-time = 100  $\mu$ s; duty factor = 0.64; voltage = 40 V)

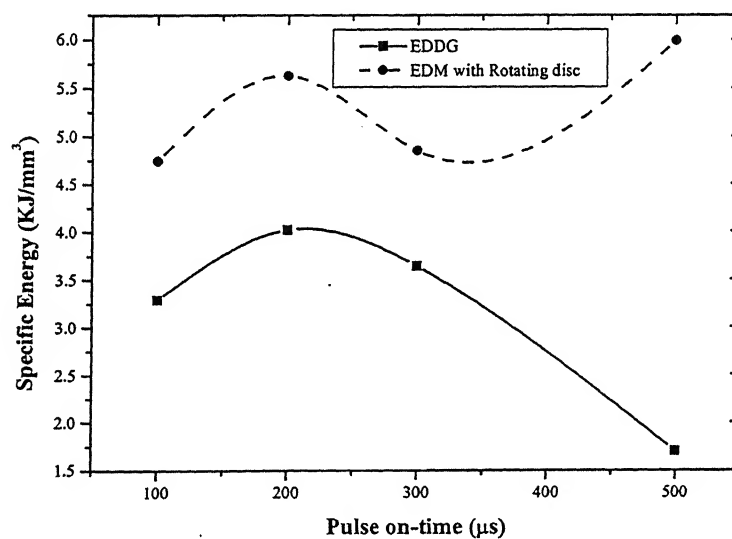


**Fig. 4.10 Specific energy in EDDG and EDM with rotating disc**  
(Pulse current = 7 A; disc speed = 2.5 m/s; duty factor = 0.64; voltage = 40 V)

Results of temperature in EDM with rotating disc and EDDG are compared below for the pulse current in the range 3 to 7A. Besides electric discharge heat source, in EDDG, abrasive action is another heat source present. So, workpiece temperature was expected to be more in case of EDDG as compared with EDM to rotating disc

temperature was expected to be more in case of EDDG as compared with EDM to rotating disc

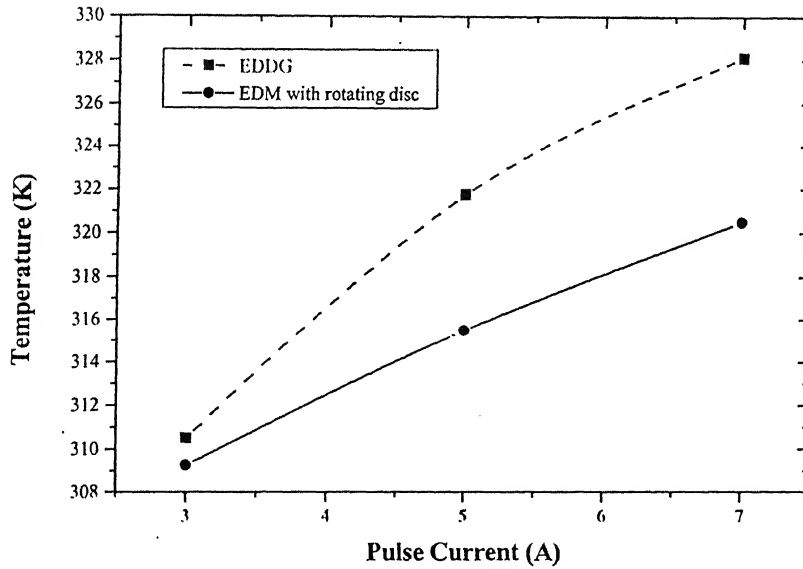


Fig. 4.11 Comparison of EDDG temperature with EDM with rotating disc (Voltage = 40 V, pulse on-time = 100  $\mu$ s, duty factor = 0.64 and wheel speed = 2.5 m/s)

Sr. No.	Process	Workpiece Material	Specific Energy (J/mm <sup>3</sup> )
1	Conventional Grinding	--	5-60 [42]
2	AFM	--	10-110 [42]
3	LBM	Mild steel	8-45 [43]
4	ECSM	--	1900-4547 [20]
5	ECG	Tool steel	85-250 [6]
6	EDM with rotating disc	HSS	4000-7000
7	EDDG	HSS	500-3000

Table 4.1 Specific energy in various processes

It is obvious from the above that EDM is very inefficient process as compared to conventional grinding, AFM and EDDG. It also underlines feasibility of EDDG to EDM with rotating disc.

# Chapter 5

## Conclusions and Scope for Future Work

---

### 5.1 Conclusions

Attempt has been made in the present work to investigate electrodischarge diamond grinding process experimentally. Experiments were conducted in two stages. Firstly, using a full factorial design, parametric analysis of process parameters (current, pulse on-time and wheel speed), with reference to the temperature of the workpiece and material removal rate, has been done. In the second stage, octagonal ring type dynamometer was employed for measurement of cutting forces. Analysis was done for evolution of cutting forces with process parameters (current, pulse on-time, duty factor, and wheel speed) and correlated with temperature. Also, specific energy in the EDDG process was evaluated and analyzed with the above mentioned process parameters. Some experiments were conducted with specially fabricated disc so as to get information about temperature and specific energy in EDM with rotating disc. A brief comparison was also made with EDDG.

Following are the specific conclusions drawn from the present thesis work.

#### ✍ Parametric analysis of EDDG

Effect of pulse current, pulse on-time and wheel speed was analyzed using  $3^3$  factorial design with temperature and MRR as responses.

- ✓ A second order regression model was found to represent relationship between input parameters and responses (temperature and MRR) significantly.
- ✓ Temperature and MRR were found to be increasing with increase in pulse current. Current is the most significant factor in affecting responses.
- ✓ MRR increases with increase in wheel speed. But, temperature was found to be decreasing with wheel speed increase. No arc instability was observed in the range of wheel speed chosen (2.5 – 7.5 m/s).
- ✓ Pulse on-time increase causes increase in both MRR and temperature. But, at 200  $\mu$ s abnormal behavior was observed.

- ✓ Wheel speed and pulse on-time shows “*anti-synergetic interaction*” . Also, pulse current and pulse current follows “*synergetic interaction*” pattern.

It can be concluded that, to achieve high MRR and low temperature rise in the workpiece, current and pulse on-time should be chosen from moderate values and wheel speed from higher values.

#### ✍ **Specific energy in EDDG**

- ✓ Cutting force decreases with increase in pulse current and pulse on-time. But, it increases with increase in wheel speed and duty factor.
- ✓ Thermal softening, grain re-sharpening, and material removal by electrical discharge action are the factors contributing to decrease in cutting forces.
- ✓ Increase in current, pulse on-time and duty factor lead to increase in specific EDDG energy. But, increase in wheel speed causes decrease in specific EDDG energy.
- ✓ Specific energy of EDDG was found to be less than that of EDM with rotating disc. It indicates that the combination of EDM and conventional grinding improves EDM process performance from the specific energy point of view.

## **5.2 Scope for Future Work**

EDDG has found enormous applications in shaping of advanced engineering materials. Complex phenomena associated with EDDG and being hybrid in nature, there is wide scope for research in this process. Present thesis work is one step towards the understanding of the process. Still, following investigations can be carried out further.

- ☞ Present study comprised of parametric analysis using three factors (current, pulse on-time and wheel speed) at a time. Use of orthogonal arrays can be made to analyze all the factors at a time provided careful selection of interactions among the factors has to be carried out.
- ☞ Hitherto experimentation was done with diamond as abrasive and bronze as a bonding material. Process performance can be studied using different types of abrasives (SiC) and bonding material (Cu).



☞ Thermal stresses are results of thermal phenomena of EDDG process. Measuring stresses with advanced techniques like X-ray diffractometer can be useful for experimental analysis of thermal stresses.

☞ Study of wheel topography is vital for technological advancement of the process. Discharge energy plays a key role in this consideration. A separate study comprising of grit protrusion and bond strength with discharge energy is needed. Also, wheel wear analysis with process parameters can be experimented.

☞ Process optimization can be tried with the use of response surface designs.

## References

1. W. KONIG, L. CRONJAGER, G. SPUR, H. TONSHOFF, M. VIGNEAU, and W. ZDEBLICK, "Machining of new materials", *Ann. CIRP*, Vol. 39(2), 673-681(1990).
2. X. YANG, and C.R. LIU, "Machining of titanium and its alloys", *Machining Science and Technology*, Vol. 3(1), pp.107-139 (1999).
3. W. KONIG, and D.F. DAUW, "EDM-Future steps towards the machining of ceramics", *CIRP Annals*, Vol. 37(2), pp.623-631 (1988).
4. F. MULLER, and J. MONAGHAN, "Non-conventional machining of particle reinforced metal matrix composite", *Int. J. Mach. Tools Manufact.*, Vol. 40, 1351-1366 (2000).
5. P.C. PANDEY and H.S. SHAN, *Modern Machining Processes*, Tata McGraw-Hill, New Delhi (1980).
6. G.F. BENEDICT, *Non Traditional Machining Processes*, Marcel Dekker (1987).
7. P. KOSHY, V.K. JAIN and G.K. LAL, "Experimental investigations into electrical discharge machining with a rotating disk electrode", *Precision Engineering*, 15(1) pp.6-15 (1993).
8. A. ERDEN and B. KAFTANOGLU, "Heat transfer modeling of electrodischarge machining", Proc. 21<sup>st</sup> Int. Machine Tool Design and Research Conference, Ed. J.M. Alexander, Macmillan, London, pp. 351-358.
9. P.C. PANDEY and S.T. JILANI, "Plasma channel growth and the resolidified layer in EDM", *Precision Engineering*, Vol. 8, No. 2, pp.104-110 (1986).
10. D. SCOTT, S. BOYINA and K.P. RAJURKAR, "Analysis and Optimization of parameter combinations in wire electrical discharge machining", *Int. J. Prod. Res.*, Vol. 29, No.11, pp. 2189-2207 (1991).

11. V. JOPELLI, D. SCOTT, K.P. RAJURKAR and R. KONDA, "Multi-objective optimization of parameters in electrical discharge machining with orbital motion of tool electrode", *Processing Adv. Matl.*, Vol. 4, pp.1-12 (1994).
12. H. OBARA, Y.TWATA and T. OSHUMI, "An attempt to detect wire temperature distribution during wire EDM", *Proc. Int. Symp. Electromachining* (1995).
13. K. ABBINSKI, K. MUSIAL, A. MIERNIKIEWICZ, S. LABZ and M. MALOTA, "Plasma temperatures in EDM", *Proc. Int. Symp. Electromachining* (1995).
14. I. INASAKI, "Grinding of hard and brittle materials", *Ann. CIRP*, Vol. 36, No. 2, pp. 463-471 (1987).
15. M.C. SHAW, *Principles of Abrasive Processing*, Oxford Science Pub. (1996).
16. T. UEDA, A. HOSOKAWA AND A. YAMAMOTO, "Studies on temperature of abrasive grains in grinding-Applications of infrared radiation pyrometer", *J. Eng. Ind.*, Vol. 107, pp. 127-133 (1985).
17. T. KATO and H. FUJII, "Temperature measurement of workpieces in conventional surface grinding", *J. Manu. Sc. Eng.*, Vol. 122, pp. 297-303 (2000)
18. J. KOZAK and K. OCZO, "Selected problems of abrasive hybrid machining", *J. Matl. Process. Tech.*, Vol. 109, pp. 360-366 (2001).
19. V. YADAVA, "Finite Element Analysis of Electrodischarge Diamond Grinding (EDDG)", *Ph.D. Thesis*, IIT Kanpur (2001).
20. A. KULKARNI, "An experimental study of discharge mechanism in ECDM", *M. Tech. thesis*, IIT Kanpur (2000).
21. T. KITAGAWA and K. MAEKAWA, "Plasma hot machining for new engineering materials", *Wear*, vol. 139, pp.251-267 (1990).
22. S. KOSHIMIZU and I. INASAKI, "Hybrid machining of hard and brittle materials", *J. Mech. Work. Tech.* Vol. 17, pp. 333-341 (1988).

23. E. YA. GRODZINSKII, "Grinding with electrical activation of the wheel surface", *Machines and Tooling*, Vol. 50, No.12, pp.10-13 (1979).
24. SH. A. BAKHTIAROV, "Efficiency of diamond wheels after contact- erosion dressing", *Stanki Instruments*, Vol. 60, No.1, pp.18-19 (1989).
25. T. AYOMA and I. INASAKI, "Hybrid machining-Combination of electrical discharge machining and grinding", *14<sup>th</sup> North American Manufacturing Research Conf., SME*, pp. 654-661 (1986).
26. K.P. RAJURKAR and B. WEI, "Abrasive electrodischarge grinding of superalloys and ceramics", *1<sup>st</sup> Int. Mach. & Grind. Conf., SME*, MR95-188 (1995).
27. P. KOSHY, V.K. JAIN and G.K. LAL, "Mechanism of material removal in electrical discharge diamond grinding", *Int. J. Mach. Tools Manufact.*, Vol. 36, No. 10, pp. 1173-1185 (1996).
28. M. GUPTA, S.K.CHOUDHURY and V.K. JAIN, "Electrical discharge diamond grinding of high speed steel", *Mach. Sc. Tech.*, Vol. 3, No. 1, pp. 91-105 (1999).
29. C. E. DAVIS, "The dependence of grinding wheel performance on dressing procedure", *Int. J. Mach. Tool Des. Res.*, Vol. 14, pp.33-52 (1974).
30. K. SUZUKI, T. UEMATSU and T. NAKAGAWA, "On-Machine trueing/dressing of metal bond grinding wheels by electrodischarge machining", *Ann. CIRP*, Vol. 36, No. 1, pp. 115-118 (1987).
31. T. TANAKA, "Affinity of diamond for metals", *Ann. CIRP*, Vol. 30, No. 1, pp. 241-245 (1981).
32. D.C. MONTGOMERY, *Design and Analysis of Experiments*, J. Wiley & Sons (1984).
33. S. H. PARK, *Robust Design and Analysis for Quality Engineering*, Chapman & Hall (1996).

34. B. LAWTON and G. KLINGENBERG, *Transient Temperature in Engineering and Science*, Oxford Uni. Press (1996).
35. M.C. SHAW, *Metal Cutting Principles*, Oxford & IBH, New Delhi (1969).
36. D. DiBITONTO, P. EUBANK, M. PATEL and M. BARRUFET, "Theoretical models of the electrical discharge machining processes", *J. Appl. Phys.*, Vol. 66, No.9, pp. 4095-4103 (1989).
37. H. DE BRUYN, "Has the delay time influence on the EDM process", *Ann. CIRP*, Vol. 31, No. 2, pp.103-106 (1982).
38. K. P. RAJURKAR and S.M. PANDIT, "Formation and ejection of EDM debris", *Trans. ASME, J. Eng. Ind.*, Vol. 108, pp. 22-26 (1986).
39. M. TOREN, Y. ZIVRIN and Y. WINOGRAD, "Melting and evaporation phenomena during electrical erosion", *Trans. ASME, J. Heat Tran.*, pp. 576-581 (1975).
40. C. RUBENSTEIN, "The mechanics of grinding", *Int. J. Mach. Tool Des. Res.*, Vol. 12, pp. 127-139 (1972).
41. F. P. BOWDEN and D. TABOR, *The Friction and Lubrication of Solids*, Oxford Uni. Press, London (1964).
42. R. K. JAIN, "Modeling and simulation of abrasive flow machining process", *Ph.D. thesis*, I.I.T. Kanpur (1999).
43. G. CHRYSSOLOURIS, *Laser Machining: Theory and Practice*, Springer-Verlag, New York, pp. 222 (1991).

# Appendix A

## Calibration Curves

---

Fig. A.1 Calibration Curve for Temperature

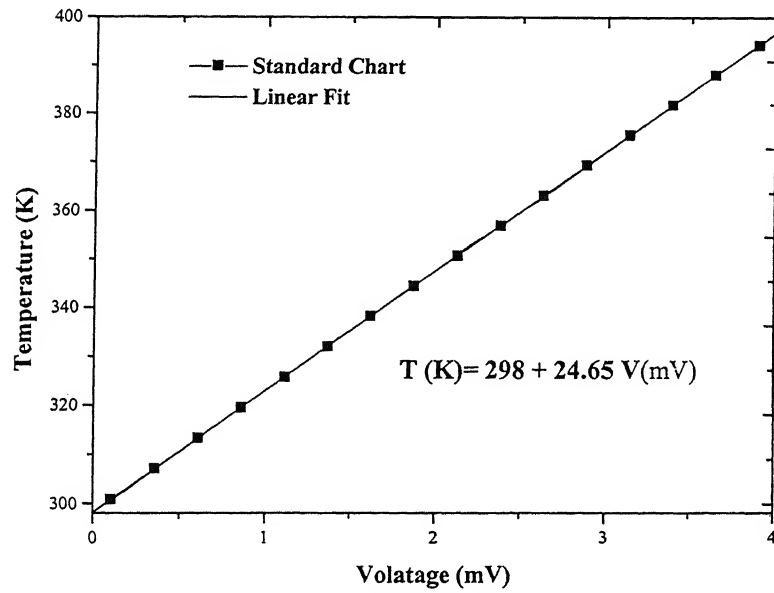
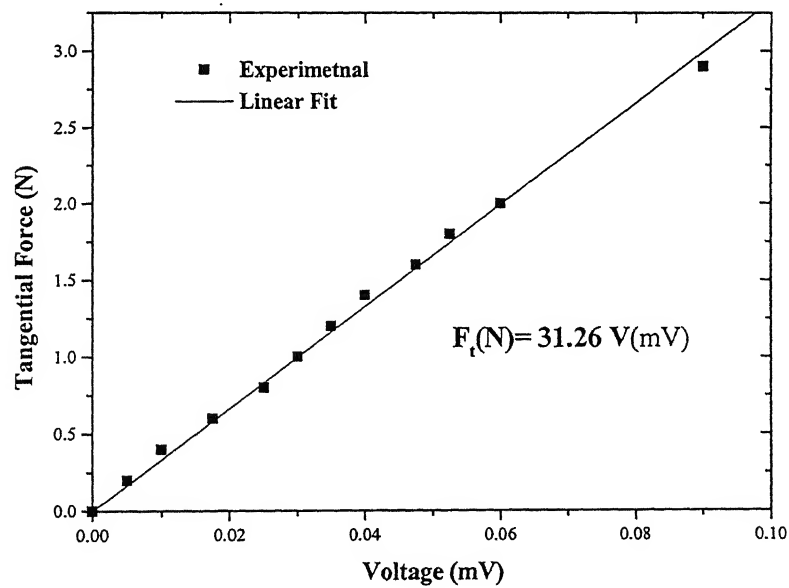
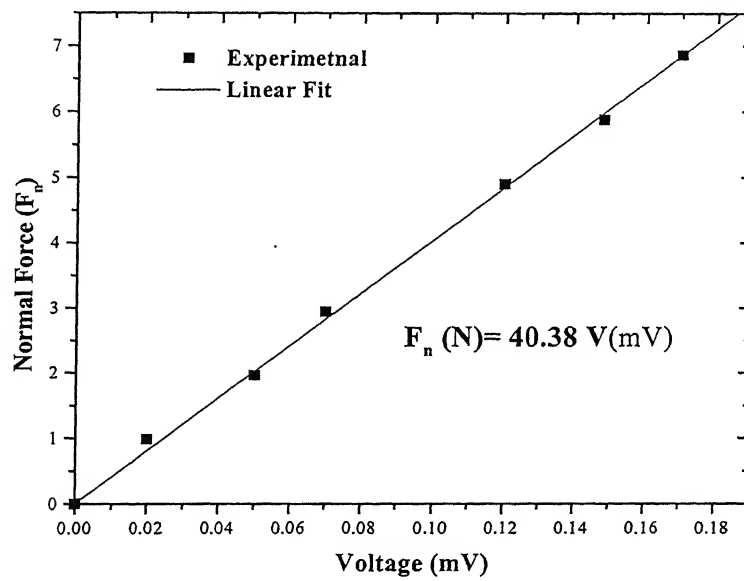


Fig. A.2 Calibration Curve for Cutting Force



**Fig. A.3 Calibration Curve for Normal Force**

# Appendix B

## Experimental Results

---

### Specific Energy in EDDG

To study the effect of pulse current on cutting forces, temperature and specific grinding energy, other parameters i.e. voltage, pulse on-time, duty cycle and wheel speed are kept at constant values. Current was varied and responses (MRR, cutting force, and temperature) were measured. All obtained data is tabulated below.

I (A)	MRR (g/min)	MRR (mm <sup>3</sup> /s)	F <sub>t</sub> (N)	P <sub>D</sub> (W)	P <sub>G</sub> (W)	Total Power (W)	Sp. EDDG Energy (KJ/mm <sup>3</sup> )	Temp. (K)
1	0.0026	0.0055	2.00	25.6	4.99	30.59	5.54	--
3	0.0200	0.0425	0.83	76.8	2.08	78.88	1.86	309.0
5	0.0220	0.0467	0.73	128.0	1.83	129.83	2.78	320.5
7	0.0259	0.0550	0.67	179.2	1.66	180.86	3.29	330.5

**Table B.1 Specific energy in EDDG with varying current**  
(Voltage = 40 V, wheel speed = 2.5 m/s, pulse on-time = 100  $\mu$ s and duty factor = 0.64)

Effect of grinding parameter i.e. cutting speed is also studied. Experiments were performed for varying speed at the same time other factors keeping at fixed values. Details of experimentation are presented in table below.

V <sub>s</sub> (m/s)	MRR (g/min)	MRR (mm <sup>3</sup> /s)	F <sub>t</sub> (N)	P <sub>D</sub> (W)	P <sub>G</sub> (W)	Total Power (W)	Sp. EDDG Energy (KJ/mm <sup>3</sup> )	Temp. (K)
1.0	0.0038	0.0081	0.50	128	0.50	128.50	15.93	347.5
2.5	0.0220	0.0467	0.73	128	1.83	129.83	2.78	320.5
5.0	0.0433	0.0919	0.83	128	4.16	132.16	1.44	310.0
7.5	0.1061	0.2253	1.16	128	8.73	136.73	0.61	304.0

**Table B.2 Specific energy in EDDG with varying wheel speed**  
(Voltage = 40 V, pulse current = 5 A, pulse on-time = 100  $\mu$ s and duty factor = 0.64)

Evolution of specific EDDG energy, cutting forces, and temperature with reference to variation in pulse on-time and duty factor are presented in Table B.3 and Table B.4, respectively.



$T_{on}$ ( $\mu s$ )	MRR (g/min)	MRR ( $mm^3/s$ )	$F_t$ (N)	$P_D$ (W)	$P_G$ (W)	Total Power (W)	Sp. EDDG Energy ( $KJ/mm^3$ )	Temp. (K)
100	0.0259	0.0550	0.67	179.2	1.68	180.88	3.29	320.5
200	0.0211	0.0448	0.33	179.2	0.83	180.03	4.02	313.0
300	0.0233	0.0495	0.25	179.2	0.62	179.82	3.64	328.0
500	0.0498	0.1057	0.17	179.2	0.42	179.62	1.70	333.0

**Table B.3 Specific energy in EDDG with varying pulse on-time**  
(Voltage = 40 V, pulse current = 7 A, duty factor = 0.64 and wheel speed = 5 m/s)

$\tau$	MRR (g/min)	MRR ( $mm^3/s$ )	$F_t$ (N)	$P_D$ (W)	$P_G$ (W)	Total Power (W)	Sp. EDDG Energy ( $KJ/mm^3$ )	Temp. (K)
0.32	0.075	0.1592	0.50	64	12.47	76.47	0.48	305.5
0.48	0.0473	0.1004	0.73	96	5.41	101.41	1.01	308.0
0.64	0.0433	0.0919	0.83	128	4.15	132.15	1.44	310.0
0.80	0.0292	0.0620	1.16	160	2.91	162.91	2.63	310.5

**Table B.4 Specific energy in EDDG with varying duty factor**  
(Voltage = 40 V, pulse current = 5 A, pulse on-time = 100  $\mu s$  and wheel speed = 5 m/s)

### Specific Energy in EDG with Rotating Disc Electrode

EDM with rotating disc is near to EDDG only difference being absence of abrasive action in later case. Comparison of EDDG with EDM with rotating disc, in the context of responses analyzed so far, can provide substantial information about betterment of EDDG.

For this purpose, to make comparison more realistic, a disc was fabricated as discussed in section 2.6. Experiments were conducted with same grinding attachment on EDM machine. Also, other settings like servo sensitivity and arc sensitivity were kept at same value as used for EDDG experimentation.

Experiments were conducted by varying current and varying pulse on-time by keeping other parameters at constant values.

I (A)	MRR (g/min)	MRR ( $mm^3/s$ )	Total Power (W)	Sp. EDM Energy ( $KJ/mm^3$ )	Temp. (K)
3	0.00573	0.0122	78.88	6.313	309.25
5	0.01000	0.0212	129.83	6.029	315.50
7	0.01780	0.0378	180.86	4.742	320.50

**Table B.5 Specific energy in EDM with rotating disc and varying current**  
 (Voltage = 40 V, duty factor = 0.64, pulse on-time = 100  $\mu$ s and wheel speed = 5 m/s)

$T_{on}$ ( $\mu$ s)	MRR (g/min)	MRR (mm <sup>3</sup> /s)	Total Power (W)	Sp. EDM Energy (KJ/mm <sup>3</sup> )	Temp. (K)
100	0.0178	0.0378	179.2	4.742	320.5
200	0.0150	0.0318	179.2	5.627	313.0
300	0.0174	0.0369	179.2	4.851	328.0
500	0.0141	0.0299	179.2	5.986	333.0

**Table B.6 Specific energy in EDM with rotating disc and varying pulse on-time**  
 (Voltage = 40 V, duty factor = 0.64, current = 7 A and wheel speed = 5 m/s)

# Appendix C

## Acronyms used in table 1.2 and 1.3

---

AM: Abrasive Machining

CHM/ CHP: Chemical Machining/ Chemical Polishing

EALBM: Etching Assisted Laser Beam Machining

EBM: Electron Beam Machining

ECAG/ECAH: Electro-Chemical Abrasive Grinding/ Electro-Chemical Abrasive Honing

ECDM/ECSM: Electro-chemical Discharge /Spark Machining

ECM: Electro- Chemical Machining

EDAG: Electro- Discharge Abrasive Grinding

EDM: Electrical Discharge Machining

EEM: Elastic Emission Machining

FFM: Fluid Flow Machining

LAE: Laser Assisted Etching

LAECM: Laser Assisted Electro- chemical Machining

LAT: Laser Assisted Turning

LBM: Laser Beam Machining

PAT: Plasma Assisted Turning

PBM: Plasma Beam Machining

UAECM: Ultrasonic Assisted Electro- chemical Machining

UAEDM: Ultrasonic Assisted Electrical Discharge Machining

UAG: Ultrasonic Assisted Grinding

UALBM: Ultrasonic Assisted Laser Beam Machining

UAP: Ultrasonic Assisted Polishing

UAT: Ultrasonic Assisted Turning